

Prepared in cooperation with the Department of the Interior WaterSMART Program

Evaluation of Statistical and Rainfall-Runoff Models for Predicting Historical Daily Streamflow Time Series in the Des Moines and Iowa River Watersheds

Scientific Investigations Report 2015–5089

Evaluation of Statistical and Rainfall-Runoff Models for Predicting Historical Daily Streamflow Time Series in the Des Moines and Iowa River Watersheds

By William H. Farmer, Rodney R. Knight, David A. Eash, Kasey J. Hutchinson, S. Mike Linhart, Daniel E. Christiansen, Stacey A. Archfield, Thomas M. Over, and Julie E. Kiang

Prepared in cooperation with the Department of the Interior WaterSMART Program

Scientific Investigations Report 2015–5089

U.S. Department of the Interior
U.S. Geological Survey

U.S. Department of the Interior
SALLY JEWELL, Secretary

U.S. Geological Survey
Suzette M. Kimball, Acting Director

U.S. Geological Survey, Reston, Virginia: 2015

For more information on the USGS—the Federal source for science about the Earth, its natural and living resources, natural hazards, and the environment—visit <http://www.usgs.gov> or call 1–888–ASK–USGS.

For an overview of USGS information products, including maps, imagery, and publications, visit <http://www.usgs.gov/pubprod/>.

Any use of trade, firm, or product names is for descriptive purposes only and does not imply endorsement by the U.S. Government.

Although this information product, for the most part, is in the public domain, it also may contain copyrighted materials as noted in the text. Permission to reproduce copyrighted items must be secured from the copyright owner.

Suggested citation:

Farmer, W.H., Knight, R.R., Eash, D.A., Hutchinson, K.J., Linhart, S.M., Christiansen, D.E., Archfield, S.A., Over, T.M., and Kiang, J.E., 2015, Evaluation of statistical and rainfall-runoff models for predicting historical daily streamflow time series in the Des Moines and Iowa River watersheds: U.S. Geological Survey Scientific Investigations Report 2015–5089, 34 p., <http://dx.doi.org/10.3133/sir20155089>.

ISSN 2328-0328 (online)

Contents

Abstract.....	1
Introduction.....	1
Purpose and Scope	2
Study Area and Data Selection	3
Methods to Estimate Daily Streamflow.....	3
Selection of Index Streamgages.....	3
Drainage-Area Ratio.....	5
Nonlinear Spatial Interpolation Using Flow Duration Curves	5
Precipitation Runoff Modeling System	5
Methods of Analysis.....	6
Results and Discussion.....	7
Summary and Conclusions.....	12
Acknowledgments.....	12
References Cited.....	13
Appendix 1. Stations Used in Analysis	15
Appendix 2. Basin Characteristics Used in Analysis	16
Appendix 3. Cross-Validation of Map Correlation.....	18
Appendix 4. Distributions of Each Performance Metric	19

Figures

1. Map showing location of the Iowa and Des Moines River Basins, study area, and landform regions in Iowa.....	2
2. Map showing location of 44 streamgages within the Iowa and Des Moines River Basins included in this study.....	4
3. Robust rank-based evaluation cloud showing the tradeoff between the mean ranking and standard deviation of the ranks of the 32 performance metrics for each method of prediction in ungaged basins.....	11
4. Graph showing for all methods of prediction in ungaged basins, the cross-site mean fraction of the validation record less than a threshold absolute percent error, a cumulative distribution of the absolute percent error.....	11
5. Graph showing for all methods of prediction in ungaged basins, the cross-site coefficient of variation of the fraction of the validation record less than a threshold absolute percent error.....	12

Appendix Figures

4-1—4-32.	Boxplots showing:	
4-1.	The distribution of the at-site Nash-Sutcliffe efficiencies of daily streamflow prediction for each method of prediction in ungaged basins (PUB).....	19
4-2.	The distribution of the at-site Nash-Sutcliffe efficiencies of the logarithms of daily streamflow predictions for each method of prediction in ungaged basins (PUB).....	19
4-3.	The distribution of the at-site root-mean-square errors of daily streamflow predictions for each method of prediction in ungaged basins (PUB).....	20
4-4.	The distribution of the at-site root-mean-square-normalized errors of daily streamflow predictions for each method of prediction in ungaged basins (PUB).....	20
4-5.	The distribution of at-site average percent errors of daily streamflow predictions for each method of prediction in ungaged basins (PUB).....	21
4-6.	The distribution of at-site Pearson correlations between simulated and observed daily streamflows for each method of prediction in ungaged basins (PUB).....	21
4-7.	The distribution of at-site Spearman correlations between simulated and observed daily streamflows for each method of prediction in ungaged basins (PUB).....	22
4-8.	The distribution of the at-site Nash-Sutcliffe efficiencies of the daily storage-yield curve (SYC) for each method of prediction in ungaged basins (PUB).....	22
4-9.	The distribution of the at-site Nash-Sutcliffe efficiencies of the logarithms of the daily storage-yield curve (SYC) for each method of prediction in ungaged basins (PUB).....	23
4-10.	The distribution of the at-site root-mean-square errors of the daily storage-yield curve for each method of prediction in ungaged basins (PUB).....	23
4-11.	The distribution of the at-site root-mean-square-normalized errors of the daily storage-yield curve for each method of prediction in ungaged basins (PUB).....	24
4-12.	The distribution of at-site average percent errors of the daily storage-yield curve for each method of prediction in ungaged basins (PUB).....	24
4-13.	The distribution of at-site Pearson correlations between the simulated and observed daily storage-yield curves for each method of prediction in ungaged basins (PUB).....	25
4-14.	The distribution of at-site Spearman correlations between the simulated and observed daily storage-yield curves for each method of prediction in ungaged basins (PUB).....	25
4-15.	The distribution of at-site percent errors in the estimated coefficient of variation of annual streamflows for each method of prediction in ungaged basins (PUB).....	26
4-16.	The distribution of at-site percent errors in the estimated coefficient of variation of daily streamflows for each method of prediction in ungaged basins (PUB).....	26

4-17.	The distribution of at-site percent errors in the estimated 10th percentile of the distribution of 7-day average annual-minimum events for each method of prediction in ungaged basins (PUB).....	27
4-18.	The distribution of at-site percent errors in the estimated 50th percentile of the distribution of 7-day average annual-minimum events for each method of prediction in ungaged basins (PUB).....	27
4-19.	The distribution of at-site percent errors in the estimated 90th percentile of the distribution of annual-maximum events for each method of prediction in ungaged basins (PUB)	28
4-20.	The distribution of at-site percent errors in the estimated 90-percent-exceedance streamflow for each method of prediction in ungaged basins (PUB).....	28
4-21.	The distribution of at-site percent errors in the estimated 75-percent-exceedance streamflow for each method of prediction in ungaged basins (PUB).....	29
4-22.	The distribution of at-site percent errors in the estimated 50-percent-exceedance streamflow for each method of prediction in ungaged basins (PUB).....	29
4-23.	The distribution of at-site percent errors in the estimated 25-percent-exceedance streamflow for each method of prediction in ungaged basins (PUB).....	30
4-24.	The distribution of at-site percent errors in the estimated 10-percent-exceedance streamflow for each method of prediction in ungaged basins (PUB).....	30
4-25.	The distribution of at-site percent errors in the estimated mean daily streamflow for each method of prediction in ungaged basins (PUB)	31
4-26.	The distribution of at-site percent errors in the estimated coefficient of variation (L-CV) of daily streamflow for each method of prediction in ungaged basins (PUB)	31
4-27.	The distribution of at-site percent errors in the estimated skewness (L-skew) of daily streamflows for each method of prediction in ungaged basins (PUB).....	32
4-28.	The distribution of at-site percent errors in the estimated kurtosis (L-kurtosis) of daily streamflows for each method of prediction in ungaged basins (PUB)	32
4-29.	The distribution of at-site percent errors in the estimated lag-1 autocorrelation of daily streamflows for each method of prediction in ungaged basins (PUB).....	33
4-30.	The distribution of at-site percent errors in the estimated amplitude of the sinusoidal seasonal trend of daily streamflows for each method of prediction in ungaged basins (PUB).....	33
4-31.	The distribution of at-site percent errors in the estimated phase of the sinusoidal seasonal trend of daily streamflows for each method of prediction in ungaged basins (PUB).....	34
4-32.	The distribution of the at-site root-mean-square-normalized errors of estimated Fundamental Daily Streamflow Statistics (FDSS) for each method of prediction in ungaged basins (PUB).....	34

Tables

1. Regional regressions of 27 flow percentiles along the daily flow duration curve for the full set of 44 streamgages in the Des Moines and Iowa Rivers.....6
2. Mean rank for each performance metric and method of prediction in ungaged basins (PUB)8
3. Standard deviation of the ranks for each performance metric and method of prediction in ungaged basins (PUB)10

Appendix Tables

1. Names, station numbers, fraction of zeros, and period of record for each streamgage used for the comparison of methods of prediction in ungaged basins in the Des Moines and Iowa River Basins.....15
2. Description of all basin characteristics considered as potential explanatory variables in the development of the regressions conducted as part of the model comparison in the Des Moines and Iowa River Basins16
3. Leave-one-out cross-validated, root-mean-squared error of the fitted variograms of intersite hydrograph correlation at 44 streamgages in the Des Moines and Iowa River Basins.....18

Conversion Factors

Multiply	By	To obtain
Length		
inch (in.)	2.54	centimeter (cm)
inch (in.)	25.4	millimeter (mm)
foot (ft)	0.3048	meter (m)
mile (mi)	1.609	kilometer (km)
square miles per mile (mi ² /mi)	1.609	square kilometers per kilometer (km ² /km)
miles per square mile (mi/mi ²)	0.6214	kilometers per square kilometer (km/km ²)
Area		
square mile (mi ²)	259.0	hectare (ha)
square mile (mi ²)	2.590	square kilometer (km ²)
Volume		
cubic foot (ft ³)	28.32	cubic decimeter (dm ³)
cubic foot (ft ³)	0.02832	cubic meter (m ³)
Flow rate		
cubic foot per second (ft ³ /s)	0.02832	cubic meter per second (m ³ /s)
Hydraulic gradient		
foot per mile (ft/mi)	0.1894	meter per kilometer (m/km)

Temperature in degrees Celsius (°C) may be converted to degrees Fahrenheit (°F) as follows:
 $^{\circ}\text{F} = (1.8 \times ^{\circ}\text{C}) + 32.$

Temperature in degrees Fahrenheit (°F) may be converted to degrees Celsius (°C) as follows:
 $^{\circ}\text{C} = (^{\circ}\text{F} - 32) + / 1.8$

Datum

Vertical coordinate information is referenced to the North American Vertical Datum of 1988 (NAVD 88).

Horizontal coordinate information is referenced to the North American Datum of 1983 (NAD 83).

Elevation, as used in this report, refers to distance above the vertical datum.

Abbreviations and Acronyms

DAR	Drainage-Area Ratio, a PUB approach. Often combined with an index selection method (NN or MC).
FA	Flow-Anywhere, a PUB approach
FDSS	Fundamental Daily Streamflow Statistics
L-CV	Second L-moment ratio
L-Skew	Third L-moment ratio
L-kurtosis	Fourth L-moment ratio
MC	Map Correlation, an index selection technique
NN	Nearest Neighbor, an index selection technique
NSE	Nash-Sutcliffe model efficiency. Also see with an appended L, denoting the use of logarithms.
PUB	Prediction in Ungaged Basins
QPPQ	Nonlinear Spatial Interpolation using Flow Duration Curves, a PUB approach. Often combined with an index selection method (NN or MC).
PRMS	Precipitation Runoff Modeling System
RRBE	Robust, Rank-Based Evaluation
RMSE	Root-Mean-Squared Error
RMSNE	Root-Mean-Squared-Normalized Error
WaterSMART	Water: Sustain and Manage America's Resources for Tomorrow

Evaluation of Statistical and Rainfall-Runoff Models for Predicting Historical Daily Streamflow Time Series in the Des Moines and Iowa River Watersheds

By William H. Farmer, Rodney R. Knight, David A. Eash, Kasey J. Hutchinson, S. Mike Linhart, Daniel E. Christiansen, Stacey A. Archfield, Thomas M. Over, and Julie E. Kiang

Abstract

Daily records of streamflow are essential to understanding hydrologic systems and managing the interactions between human and natural systems. Many watersheds and locations lack streamgages to provide accurate and reliable records of daily streamflow. In such ungaged watersheds, statistical tools and rainfall-runoff models are used to estimate daily streamflow. Previous work compared 19 different techniques for predicting daily streamflow records in the southeastern United States. Here, five of the better-performing methods are compared in a different hydroclimatic region of the United States, in Iowa. The methods fall into three classes: (1) drainage-area ratio methods, (2) nonlinear spatial interpolations using flow duration curves, and (3) mechanistic rainfall-runoff models. The first two classes are each applied with nearest-neighbor and map-correlated index streamgages. Using a threefold validation and robust rank-based evaluation, the methods are assessed for overall goodness of fit of the hydrograph of daily streamflow, the ability to reproduce a daily, no-fail storage-yield curve, and the ability to reproduce key streamflow statistics. As in the Southeast study, a nonlinear spatial interpolation of daily streamflow using flow duration curves is found to be a method with the best predictive accuracy. Comparisons with previous work in Iowa show that the accuracy of mechanistic models with at-site calibration is substantially degraded in the ungaged framework.

Introduction

Daily records of streamflow provide foundational records of hydrologic processes within gaged watersheds. These records are essential to a hydrologic understanding of natural systems. Furthermore, these records help in understanding how human systems intersect with and affect natural systems. An informed hydrologic understanding affects the

ability to protect natural resources, design water abstractions for drinking or irrigation, develop hydropower resources, and protect against hydrologic extremes (Sivapalan, 2003; Sivapalan and others, 2003; Vogel, 2011; Hrachowitz and others, 2013). Unfortunately, the ability to collect long-range streamflow records is constrained by time and resources; as a result, the national network of streamgages is both spatially and temporally sparse (Kiang and others, 2013). For this reason, the exploration of tools for the prediction or estimation of daily streamflow records in unmonitored or ungaged locations is essential for an improved hydrologic understanding.

The problem of prediction in ungaged basins (PUB) has become an international research question (Sivapalan and others, 2003; Viglione and others, 2013). In the United States, the PUB problem has been of pivotal importance for initiatives like WaterSMART (Sustain and Manage America's Resources for Tomorrow; [Salazar, 2010; Alley and others, 2013]) and the U.S. Geological Survey's National Water Census (U.S. Geological Survey, 2007; Alley and others, 2013). The National Water Census seeks to provide spatially and temporally continuous records of daily streamflow across the United States, an endeavor that necessitates an immense amount of PUB. The work presented in this report is directly supported by the National Water Census and serves as a second case study of PUB methods in the United States.

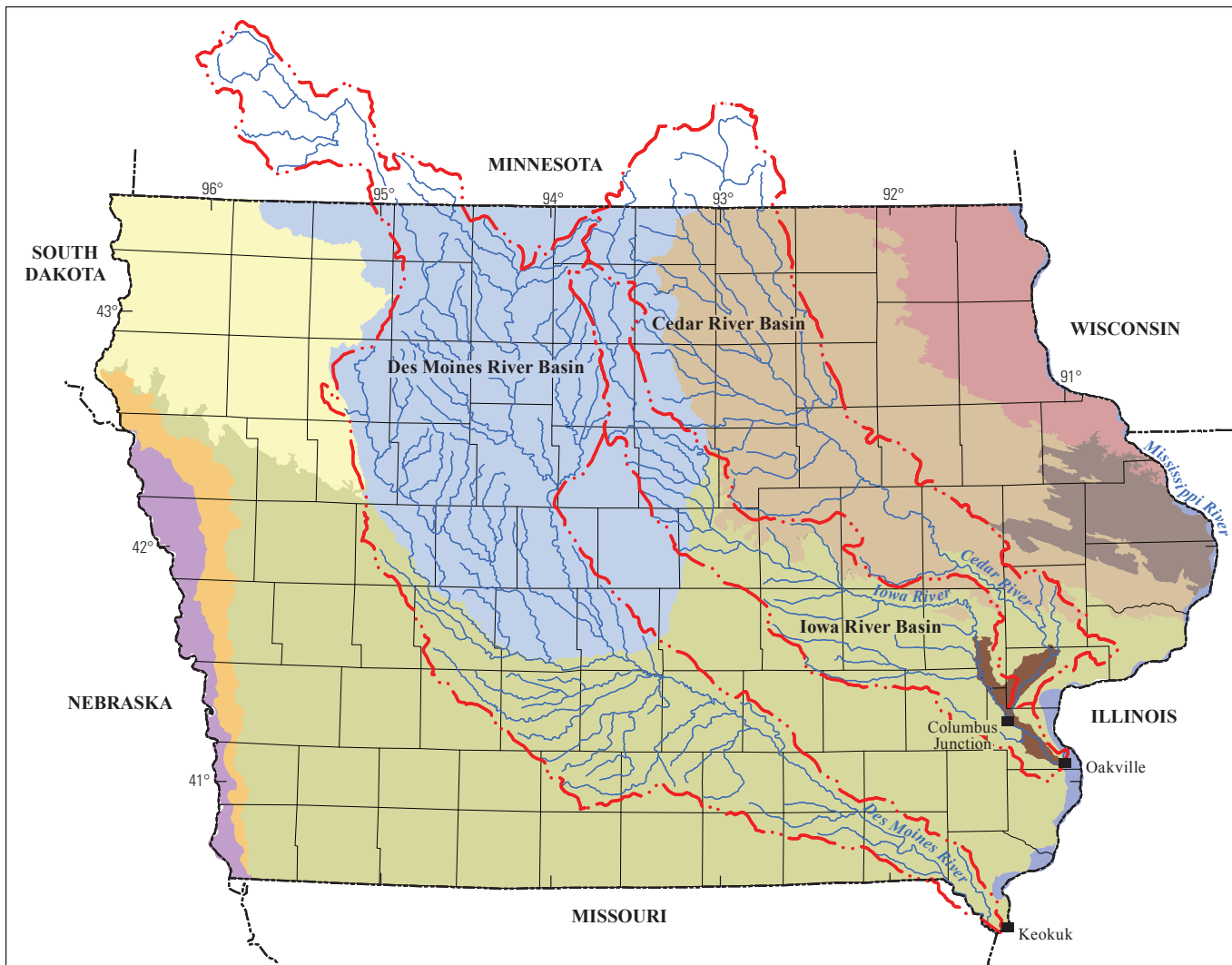
Recently, Farmer and others (2014) completed an exploration of PUB methods in the southeastern United States. There, 19 variations of PUB methods were compared to estimate 30-year records of daily streamflow. Considering a wide-range of performance metrics, results indicated that several PUB methods performed reasonably well. On average, a transfer and transformation of flow duration curves served as the best approach to predicting daily streamflow records. The Southeast is a fairly humid region with generally homogeneous climate. Trends in precipitation and temperature are largely driven by elevation. The purpose of this report is to consider a similar model comparison in another hydroclimatic region.

2 Evaluation of Statistical and Rainfall-Runoff Models in the Des Moines and Iowa River Watersheds

After the Southeast study (Farmer and other, 2014), the Des Moines and Iowa Rivers in Iowa were identified as another case study. The legacy of model comparison (Linhart and others, 2011 and 2013) allows for historical comparison as well as the implementation of newer tools. Iowa is substantially smaller than the southeastern region, but presents a number of other challenges: a different hydroclimatic regime, less variation in elevation, and a variety of different landform regions (Prior and others, 2009). The purpose of this Iowa model comparison presented in this report is to explore the advantages and disadvantages of several PUB methods that performed well in the Southeast model comparison.

Purpose and Scope

This report presents a comparison of five different methods for predicting continuous daily records of streamflow in the Des Moines and Iowa River Basins (fig. 1). Each prediction method is assessed for its overall accuracy of predicting a hydrograph of daily discharge, its ability to reproduce daily, no-fail storage yield curves, and its ability to reproduce key observed streamflow statistics. Hydrographs of daily discharge are estimated at 44 sites from October 1, 1983, through September 30, 2011. The PUB methods are compared using Robust Rank-Based Evaluation and the cumulative



Base from U.S. Geological Survey digital data,
1:2,000,000, 1979
Universal Transverse Mercator projection,
Zone 15
North American Datum of 1983 (NAD 83)

0 25 50 MILES
0 25 50 KILOMETERS

EXPLANATION

 Des Moines Lobe	 Mississippi River Alluvial Plain
 East-Central Iowa Drift Plain	 Missouri River Alluvial Plain
 Iowa-Cedar Lowland	 Northwest Iowa Plains
 Iowan Surface	 Paleozoic Plateau
 Loess Hills	 Southern Iowa Drift Plain

Figure 1. Location of the Iowa and Des Moines River Basins, study area, and landform regions in Iowa.

distribution of absolute errors. The results provide a complement to the Southeast model comparison. The purpose of the Iowa model comparison presented in this report is to, in a different hydroclimatic region, to explore the advantages and disadvantages of several PUB methods that performed well in the Southeast model comparison.

Study Area and Data Selection

The Iowa and Des Moines Rivers generally flow in a southeasterly direction to join the Mississippi River along the eastern border of Iowa (fig. 1). (A list of all streamgages evaluated in this study is included in Appendix 1) The Iowa River Basin drains approximately 12,640 square miles at the confluence with the Mississippi River near Oakville, Iowa. This includes the Cedar River Basin, which constitutes approximately 62 percent of the Iowa River Basin (Larimer, 1957). The Cedar River Basin extends from its headwaters in southern Minnesota to its confluence with the Iowa River near Columbus Junction in east-central Iowa. The Des Moines River Basin drains almost 14,700 square miles at the confluence with the Mississippi River near Keokuk, Iowa (Larimer, 1957). Collectively, the Iowa and Des Moines River Basins drain approximately 27,300 square miles at their respective confluences with the Mississippi River. The Iowa and Des Moines River Basins cross 5 of the 10 distinct landform regions in Iowa (Prior and others, 2009), including the Des Moines Lobe, the Iowan Surface, the Southern Iowa Drift Plain, and the Iowa-Cedar Lowland, with a small portion of the Des Moines River Basin draining the Northwest Iowa Plains.

The dominant land use in the Des Moines and Iowa River Basins is row-crop agriculture (67 and 73 percent, respectively). Corn and soybean production represents approximately 60 percent of the row-crop agriculture, with the remaining portion distributed across noncropland covers (Falcone, 2011). Artificial drainage networks, including subsurface tile and open ditches, are extensively used in Iowa to remove excess water and support row-crop agriculture. Other land use throughout these basins includes confined and unconfined livestock operations for beef and dairy cattle, hogs, sheep, and poultry (Iowa Department of Natural Resources, 2006). For the period from 1971 to 2000 average annual precipitation was 33 inches in the Des Moines Basin and 34.7 inches in the Iowa River Basin. Average annual temperature for the same period in the Des Moines River Basin was 47.6 °Fahrenheit (F) (minimum of 37.2 °F; maximum of 58.73 °F), while the average annual temperature in the Iowa River Basin was 47 °F (minimum of 36.9 °F; maximum of 57.9 °F) (Falcone, 2011).

This study uses the same 44 streamgages in the Iowa and Des Moines River Basins that were used in a previous state-wide comparison of PUB methods in Iowa (Linhart and others, 2012). The locations of the 44 streamgages are shown in figure 2. Appendix 2 lists the basin-characteristic values that were measured for these 44 streamgages as part of a peak-flow study for Iowa (Eash and others, 2013) and were used for the development of 27 regression equations in this study.

Methods to Estimate Daily Streamflow

Three approaches to PUB were used to estimate daily streamflow records, including a drainage-area ratio method, a nonlinear spatial interpolation using flow duration curves, and the Precipitation Runoff Modeling System (PRMS). The former two are direct-transfer, statistical models that do not explicitly rely on a process-understanding of basin hydrology. The PRMS, on the other hand, models the physical processes of streamflow generation in gaged basins and transfers that physical understanding to ungaged locations. All methods require the selection of an index streamgage from which to transfer the physical or statistical understanding to the ungaged location. Two techniques for the selection of index streamgages, nearest neighbor and map correlation, were used. A description of the index selection techniques and PUB approaches are provided in the Selection of Index Streamgages section of this report. The coupling of an index-selection technique and a PUB approach, both of which are required to produce estimates of streamflow, is termed a PUB method. Farmer and others (2014) and Farmer (2015) implemented these methods in the southeastern United States and provide further information on the development and application of these methods.

Selection of Index Streamgages

All of the PUB approaches considered here require the selection of an index streamgage from which to transfer hydrologic information to an ungaged location. Two techniques for the selection of index streamgages, nearest neighbor and map correlation, were used for each of the direct-transfer, statistical approaches, drainage area ratio-, and nonlinear spatial interpolation using flow duration curves. A modified version of the nearest-neighbor selection technique was used with the PRMS. The combinations of index selection techniques and PUB approaches define five PUB methods and yields five unique estimates of daily streamflow at each location.

An index streamgage is any streamgage from which hydrologic information is transferred. In the nearest-neighbor technique, the optimal index streamgage is the streamgage geographically closest to the ungaged location of interest. Map correlation (Archfield and Vogel, 2010) uses geostatistical tools to identify the streamgage with the greatest estimated correlation with the anticipated daily record at the ungaged location and selects it as the optimal index streamgage. As described by Archfield and Vogel (2010), map correlation proceeds by fitting a regional variogram for each site in the network. Each variogram, which is tied to a specific site, estimates the Pearson correlation coefficient between the streamflow at the linked site and the records at any other location. By inputting the coordinates of the an ungaged site into each of the site-specific variograms, it is possible to determine which network streamgage is expected to provide the greatest level of correlation with the ungaged site; this site is selected as the optimal index streamgage. (Appendix 3 provides the leave-one-out validation root-mean-squared errors of map correlation, indicating the applicability

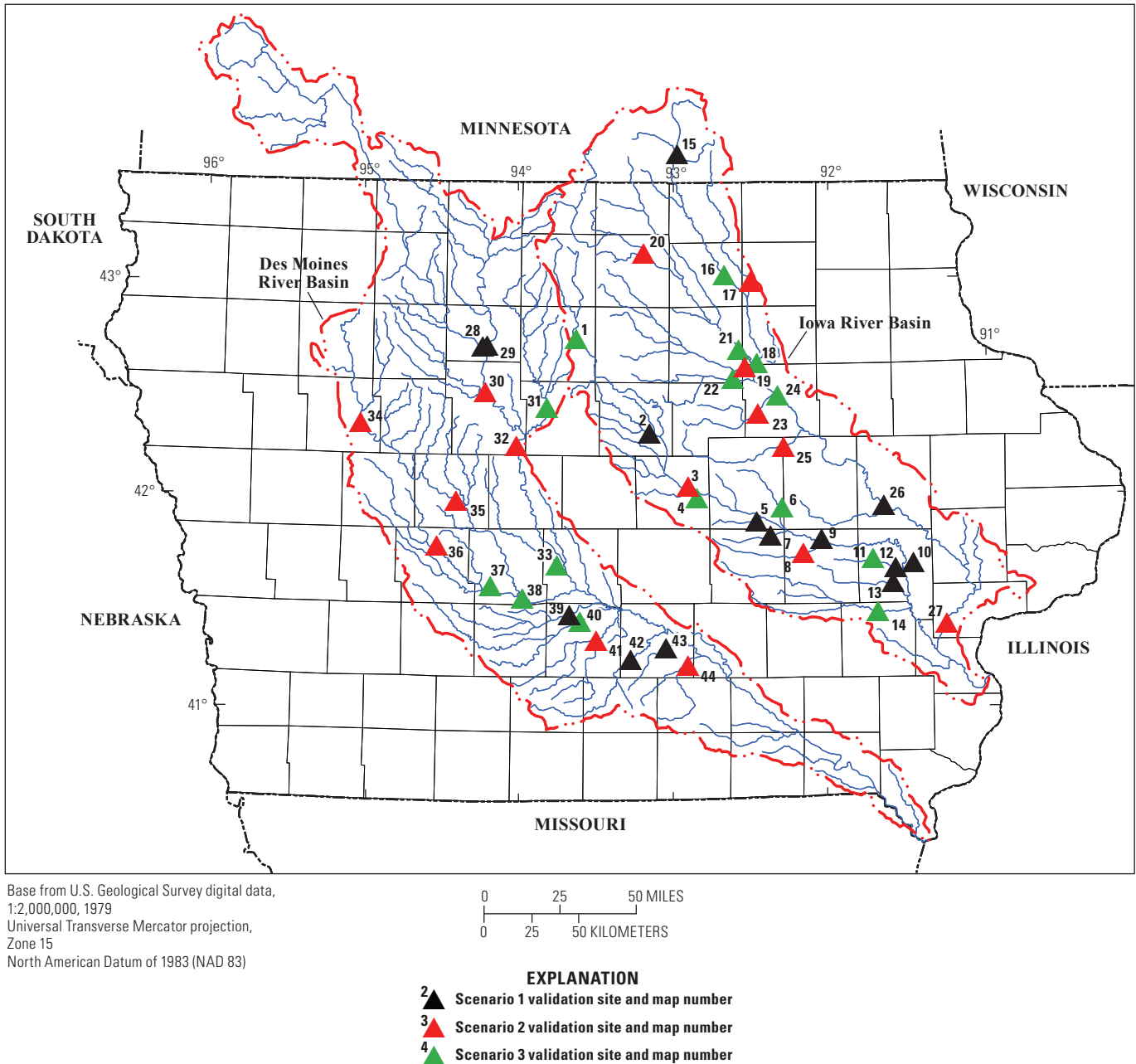


Figure 2. Location of 44 streamgages within the Iowa and Des Moines River Basins included in this study.

of this index streamgauge selection technique in this region. The average root-mean-squared error is 0.0274.) For both nearest neighbor and map correlation, the location of each stream site, gaged or ungaged, is defined by the latitude and longitude of the basin outlet. Both nearest neighbor and map correlation were coupled with each of the direct-transfer statistical methods. For the PRMS, the nearest-neighbor procedure was amended: Only streamgages with an at-site calibration of the PRMS producing a Nash-Sutcliffe model efficiency (Nash and Sutcliffe, 1970) greater than 0.80 were considered as potential index streamgages. From this subset of streamgages, the optimal index streamgauge was selected by spatial proximity.

Unlike the PRMS, which transfers model parameters rather than time series, the direct-transfer, statistical PUB approaches require observations from an index streamgauge for each day of prediction. If the most optimal index streamgauge, based on spatial proximity or estimated correlation, is not operational on the target date, then an alternative must be selected for that date. This was accomplished by ranking the potential index streamgages based on spatial proximity or estimated correlation. Farmer and others (2014) provide an illustrative example. The date-range gaps are then filled by working successively down the ranked population of potential index streamgages.

Drainage-Area Ratio

The prediction of streamflow records using the drainage-area ratio (DAR) PUB approach has been widely practiced in the fields of hydrology and water resources engineering (Hirsch, 1979; Asquith and others, 2006). The DAR method is predicated on the assumption that streamflow per unit area is equivalent across hydrologically similar sites. Hydrologic similarity can be defined several ways; here it is approximated by the selection of an optimal index streamgauge. With an index streamgauge, the ungaged streamflow on day t can be approximated as:

$$\hat{Q}_{u,t} = \frac{A_u}{A_g} \cdot Q_{g,t} \quad (1)$$

where $\hat{Q}_{u,t}$ is the estimated streamflow at the ungaged location on day t , $Q_{g,t}$ is the corresponding measured streamflow at the index streamgauge and A_u and A_g are the drainage areas associated with the ungaged and gaged locations, respectively. The DAR approach is the foundation for the Flow Anywhere method presented and assessed by Linhart and others (2012). Here, the application of DAR with nearest-neighbor index streamgages is noted as DAR-NN, while the application with map-correlation index streamgages is noted as DAR-MC.

Nonlinear Spatial Interpolation Using Flow Duration Curves

Where the DAR approach seeks to scale the daily streamflow by drainage area, the approach of nonlinear spatial interpolation using flow duration curves can be thought of as a statistical scaling of the entire flow duration curve at each site. This approach has been widely used (Fennessey, 1994; Hughes and Smakhtin, 1996; Smakhtin, 1999; Mohamoud, 2008; Archfield and others, 2010; Shu and Ouarda, 2012) and shown to perform well across a range of performance metrics (Farmer and others, 2014). As noted by Farmer and others (2014), this approach has gone by many names; here the nearest-neighbor implementation is abbreviated QPPQ-NN, while the map-correlation implementation is noted as QPPQ-MC. The abbreviation of QPPQ, as described in the next paragraph, refers to the use of an index discharge (Q) to produce an index probability (p), which yields an estimated, ungaged probability (p) and produces an estimate of ungaged discharge (Q).

QPPQ predicts ungaged streamflow records by assuming that the exceedance probabilities of streamflow on a particular day are identical between two hydrologically similar sites:

$$P_{u,t} = P(Q_u \geq Q_{u,t}) = P(Q_g \geq Q_{g,t}) = P_{g,t} \quad (2)$$

where $Q_{u,t}$ and $Q_{g,t}$ are the ungaged and index streamflows on day t , respectively, and $P_{u,t}$ and $P_{g,t}$ are the complementary cumulative probabilities (or exceedance probabilities) of the

ungaged and index streamflow. By this method, the streamflow at the index streamgauge ($Q_{g,t}$) is converted to a complimentary cumulative probability ($P_{g,t}$) using an empirical flow duration curve. Using the assumption of equation (2), this exceedance probability is then transferred to the ungaged site as an estimate of the ungaged complimentary cumulative probability ($\hat{P}_{u,t}$). The estimate exceedance probability is then converted into an estimate of ungaged streamflow ($\hat{Q}_{u,t}$) by means of an estimated flow-duration curve at the ungaged site.

For this application of QPPQ, as in Farmer and others (2014), the estimated flow duration curve at the ungaged site was obtained by regional regressions of 27 key exceedance probabilities. The exceedance probabilities considered were 0.02, 0.05, 0.1, 0.2, 0.5, 1, 2, 5, 10, 20, 25, 30, 40, 50, 60, 70, 75, 80, 90, 95, 98, 99, 99.5, 99.8, 99.9, 99.95, and 99.98 percent. Defining the entire study area as a single region, regional regressions for each exceedance probability were developed in the same way as Farmer and others (2014): The streamflow quantiles associated with each exceedance probability at each gaged location were identified empirically using the Blom plotting position (Stedinger and others, 1983). Several basin characteristics (Appendix 2) were considered as explanatory variables in a log-linear regression framework. The best regional regressions for each quantile are summarized in table 1. Using these regressions, the 27 quantiles composing the flow-duration curve were estimated at an ungaged site. In the prediction of streamflow values, log-linear interpolation was used for estimated exceedance probabilities falling between any two of the 27 exceedance probabilities. For extrapolations beyond the 27 exceedance probabilities, streamflows with complimentary cumulative probabilities less than 0.02 percent and more than 99.98 percent, the QPPQ approach defaulted to the DAR approach. Additional details on the development of this regression approach are provided in Farmer and others (2014).

Precipitation Runoff Modeling System

Unlike the statistical approaches, DAR and QPPQ, the Precipitation-Runoff Modeling System (PRMS; Leavesley and others, 1983; Markstrom and others, 2008; 2014) provides a physically-based, mechanistic model of streamflow. As described in Farmer and others (2014), the PRMS is a modular, deterministic, distributed-parameter watershed model that was designed to simulate, as driven by climatic inputs, land-surface hydrologic processes and water budgets at various temporal scales. The PRMS models aggregate watersheds by representing individual stream segments and unique, homogeneous hydrologic response units. The PRMS was calibrated for gaged watersheds using the Shuffled Complex Evolution algorithm (Duan and others, 1992, 1993, and 1994), which allowed adjustment of the initial calibration parameters derived from basin characteristics to account for the idiosyncrasies of specific hydrologic response units. In ungaged basins, the adjustments from initial parameters, as opposed to the

6 Evaluation of Statistical and Rainfall-Runoff Models in the Des Moines and Iowa River Watersheds

Table 1. Regional regressions of 27 flow percentiles along the daily flow duration curve for the full set of 44 streamgages in the Des Moines and Iowa Rivers.

[NA, not applicable. Shaded rows indicate left-censored regression. Basin characteristics considered as potential explanatory variables are listed in Appendix 2]

Flow percentile (percent)	Equation	Number of censored streamgages	Standard error of prediction (percent)	Standard error of estimate divided by root-mean-squared error (percent)
0.02	$10^{-2.201} \text{DRNAREA}^{0.760} \text{JULYAVEPRE}^{6.520} \text{CCM}^{-0.507}$	0	19.04	18.23
0.05	$10^{-2.114} \text{DRNAREA}^{0.770} \text{JULYAVEPRE}^{6.431} (\text{DESMOIN}+1)^{-0.064}$	0	13.11	12.57
0.1	$10^{-3.049} \text{DRNAREA}^{0.763} \text{JULYAVEPRE}^{5.827} \text{CLAY}^{0.835}$	0	14.12	13.52
0.2	$10^{-3.097} \text{DRNAREA}^{0.798} \text{JULYAVEPRE}^{5.511} \text{CLAY}^{-0.875}$	0	12.63	12.10
0.5	$10^{-2.704} \text{DRNAREA}^{0.842} \text{JULYAVEPRE}^{4.316} \text{CLAY}^{-0.950}$	0	11.40	10.92
1	$10^{-0.805} \text{DRNAREA}^{0.882} 10^{0.368}(\text{JULYAVEPRE}) 10^{0.014}(\text{CLAY})$	0	11.78	11.28
2	$10^{-0.642} \text{DRNAREA}^{0.926} 10^{0.289}(\text{JULYAVEPRE}) 10^{0.011}(\text{CLAY})$	0	11.91	11.40
5	$10^{-0.028} \text{DRNAREA}^{0.967} 10^{0.117}(\text{JUNEAVPRE}) 10^{0.013}(\text{SOILD})$	0	9.16	8.79
10	$10^{-0.462} \text{DRNAREA}^{1.019} \text{SOILC}^{-0.053} \text{PRC8}^{1.103}$	0	8.65	8.29
20	$10^{-0.481} \text{DRNAREA}^{1.020} 10^{-0.003}(\text{SOILC}) 10^{0.110}(\text{PRC8})$	0	8.57	8.21
25	$10^{-0.654} \text{DRNAREA}^{1.017} 10^{-0.004}(\text{SOILC}) 10^{0.131}(\text{PRC8})$	0	8.64	8.27
30	$10^{-0.857} \text{DRNAREA}^{1.022} 10^{-0.004}(\text{SOILC}) 10^{0.155}(\text{PRC8})$	0	8.86	8.48
40	$10^{-1.221} \text{DRNAREA}^{1.028} 10^{-0.004}(\text{SOILC}) 10^{0.199}(\text{PRC8})$	0	11.40	10.90
50	$10^{-1.281} \text{DRNAREA}^{1.027} 10^{0.018}(\text{HYSEP}) 10^{-0.320}(\text{CCM})$	0	14.60	14.00
60	$10^{-1.684} \text{DRNAREA}^{1.047} 10^{0.023}(\text{HYSEP}) 10^{-0.421}(\text{CCM})$	0	18.90	18.10
70	$10^{-2.379} \text{DRNAREA}^{1.089} 10^{0.028}(\text{HYSEP}) 10^{-0.003}(\text{DESMOIN})$	0	21.96	21.04
75	$10^{-2.678} \text{DRNAREA}^{1.126} 10^{0.030}(\text{HYSEP}) 10^{-0.004}(\text{DESMOIN})$	0	25.15	24.09
80	$10^{0.534} \text{DRNAREA}^{1.125} 10^{-3.148}(\text{STREAM_VAR}) (\text{SOILD}+1)^{-0.202}$	0	29.52	28.23
90	$10^{-3.636} \text{DRNAREA}^{1.281} 10^{3.445}(\text{BFI}) 10^{-0.005}(\text{DESMOIN})$	0	43.41	41.47
95	$10^{-6.699} \text{DRNAREA}^{1.244} 10^{0.086}(\text{TAU}) 10^{0.512}(\text{JUNEAVPRE})$	0	59.44	56.68
98	$10^{-6.963} \text{DRNAREA}^{1.301} 10^{0.095}(\text{TAU}) 10^{0.443}(\text{JUNEAVPRE})$	2	NA	66.11
99	$10^{-5.038} \text{DRNAREA}^{1.320} 10^{0.093}(\text{TAU}) 10^{0.049}(\text{SOILA})$	2	NA	78.82
99.5	$10^{-5.214} \text{DRNAREA}^{1.301} 10^{0.096}(\text{TAU}) (\text{SOILA}+1)^{0.423}$	3	NA	86.40
99.8	$10^{-11.562} \text{DRNAREA}^{1.306} \text{TAU}^{6.161} (\text{SOILA}+1)^{0.472}$	3	NA	90.53
99.9	$10^{-12.636} \text{DRNAREA}^{1.301} \text{TAU}^{6.852} (\text{SOILA}+1)^{0.552}$	6	NA	109.86
99.95	$10^{0.368} \text{DRNAREA}^{1.377} 10^{-6.138}(\text{STREAM_VAR})$	6	NA	116.00
99.98	$10^{0.374} \text{DRNAREA}^{1.403} 10^{-6.380}(\text{STREAM_VAR})$	8	NA	129.70

parameter values themselves, were transferred from the index streamgage and used to adjust the initial parameters in the ungaged watershed. Farmer and others (2014) provide a more detailed description of this ungaged application of the PRMS; their approach was followed in this report. This approach is only a first-order approach to the application of the PRMS in ungaged watersheds and differs significantly from the at-site calibrated application of Linhart and others (2013).

Methods of Analysis

The performance of the PUB methods was assessed using robust rank-based evaluation (RRBE), a technique presented in Farmer and others (2014) and refined in Farmer (2015). RRBE blends several measures of performance to provide a broad assessment of the relative accuracy of streamflow predictions. This model comparison of PUB methods in Iowa considered the same goodness-of-fit metrics used by Farmer and others (2014). Additionally, the cumulative distributions of daily percent errors were used to further distinguish

between PUB methods. All analyses were conducted using a threefold validation: two-thirds of the sites were used to calibrate the PUB methods used to predict streamflow at the remaining, validation one-third of the sites. In this manner, the neglected one-third of the network is modeled without any effect from the calibration, just as if it were truly ungaged. The calibration and validation sets were iterated so that an ungaged estimate was created for each site. The definitions of scenarios are provided in figure 2, with particular streamgages noted in Appendix 1.

Thirty-two performance metrics were used for the RRBE. The overall goodness of fit was assessed with seven metrics, including the Nash-Sutcliffe of the untransformed (NSE) and natural-logarithmically transformed (NSEL) streamflow predictions, the root-mean-square error in streamflow predictions (RMSE), the root-mean-square-normalized error in streamflow predictions (RMSNE), the average percent error in streamflow estimates, the Pearson correlation coefficient between observed and predicted streamflow and the Spearman correlation coefficient between observed and predicted streamflow. The daily, no-fail storage-yield curve indicates how much storage would be required, given historical properties

of streamflow, to produce a constant yield from the stream. As an indication of streamflow signature, the reproducibility of the daily, no-fail storage-yield curve was assessed by applying the same seven metrics to predictions of the daily, no-fail storage. Farmer and others (2014) detail how the daily, no-fail storage-yield curve was estimated. In addition to overall goodness of fit and streamflow signature, the reproducibility of several streamflow statistics was assessed by observing the ratio of estimated to observed streamflow statistics; these statistics included the coefficient of variation of annual streamflow, the coefficient of variation of daily streamflow, the 10th and 50th percentiles of the empirical distribution of 7-day-average annual minimum flows, the 90th percentile of the empirical distribution of annual maximum flows, the 10th, 25th, 50th, 75th and 90th percentiles of the distribution of daily streamflow (note that annual minima and maxima were assessed using empirical distributions; no parametric fitting was applied). This analysis also considered the reproducibility of the seven fundamental daily streamflow statistics, consisting of the mean streamflow, coefficient of variation as an L-moment ratio (L-CV), skewness (L-skew), kurtosis (L-kurtosis) and autoregressive lag-one autocorrelation coefficient of daily streamflow, and the amplitude and the phase of the sinusoidal seasonal signal (Archfield and others, 2013). To strengthen the weight of the fundamental daily streamflow statistics, a RMSNE was calculated across all seven statistics. Despite the strong correlation between some performance metrics, like the RMSE and NSE, these metrics were included because they are commonly considered and quantify extremely important aspects of the model performance. As reported by Farmer and others (2014), this did not hamper the analysis, but alternative collections of metrics can be similarly compared.

The performance metrics were computed only on complete water years between October 1, 1982 and September 30, 2011. Zero-flows were included with a censoring value. Most of the statistics used complete water years, but the two percentiles of the distribution of the 7-day-average annual minimum flow were computed with complete climatic years. Climatic years are defined such that they begin on April 1 and end on March 31. (The year between April 1, 1983 and March 31, 1984, is referred to as the 1984 climatic year.) Because the percent errors and logarithmic performance metrics cannot be applied to zero-valued flows, the zero value was censored. The smallest non-zero flow published by the U.S. Geological Survey (USGS) is 0.01 cubic foot per second (ft^3/s). For this reason, any predictions on the inclusive range between 0.005 and 0.01 ft^3/s were corrected to 0.01 ft^3/s . Predictions less than 0.005 ft^3/s were set to a censored value of 0.001 ft^3/s . Observations of 0 ft^3/s were censored to 0.001 ft^3/s . While the choice of a censoring value may affect the performance metrics, only 0.07 percent of all the days at all the sites had observations with a streamflow value of zero. This fraction was considered to be small enough so as not to significantly affect the analysis.

RRBE combines the relative rankings of the PUB methods according to each performance metric. For a particular performance metric at a particular site, the five PUB methods were ranked, with best method receiving the lowest rank. Ties were ranked identically with the lowest numerical ranking available. This process was repeated for each site. The ranks for a particular PUB method were summarized across all sites, taking the average ranking and the standard deviation of the ranks. This ranking procedure was then conducted for each additional performance metric. The result was an average ranking and standard deviation of the ranks of each PUB method for each performance metric. Each PUB method can then be represented as a cloud of points in Cartesian space with the cross-site average ranking for each metric on one axis and the cross-site standard deviation of the ranks for each metric on the other axis. For a particular PUB method, this cloud of performance metrics can be summarized by averaging to obtain the centroid of the cloud. An indication of the spread of this cloud, for a particular PUB method, can be obtained by wrapping a variability ellipse around the centroid. The axes of the ellipse are defined by the cross-metric standard deviation among the cross-site averages and the cross-site standard deviations. Farmer (2015) provides examples of this analysis. The most optimal PUB methods are those with a centroid closest to the origin, representing the best average cross-site ranking and the least cross-site variability. Furthermore, the ideal method should have a smaller variability ellipse, indicating only a low level of variability across performance metrics.

The cumulative distribution of absolute percent errors in daily streamflow gives an indication of the degree of error in streamflow predictions from a particular PUB method. At a particular site, the absolute percent error of each day in the validation record was calculated (the validation record refers to complete water years for which observations and predictions are available). The distribution of errors is represented as the fraction of the validation record below a certain threshold. The cumulative distribution is obtained by increasing the threshold. The best PUB methods would show a steep rise in the percentage of record below an error threshold for low threshold values. This analysis was conducted for all sites in the study and the mean percent of the record below a threshold was documented. Because of the use of error thresholds, this technique is referred to herein as a threshold analysis.

Results and Discussion

The mean of the ranks of each PUB method according to each performance metric are shown in table 2. (The distributions of each performance metric are provided in Appendix 4.) Except for some metrics where the map-correlation (MC) application of QPPQ is marginally better when compared to its nearest-neighbor (NN) complement, the nearest-neighbor applications have a better average ranking. QPPQ-MC performed better than QPPQ-NN in

Table 2. Mean rank for each performance metric and method of prediction in ungaged basins (PUB).

[At each site, the PUB methods were ranked according to a single metric, with the best method receiving the lowest rank. These ranks were then averaged across sites for each PUB method. The process was repeated for each of the 32 metrics and 5 PUB methods. The PUB methods include the Precipitation Runoff Modeling System (PRMS), drainage-area ratio with the nearest-neighboring index streamgage (DAR-NN) or the map-correlated index streamgage (DAR-MC) and nonlinear spatial interpolation using flow duration curves with the same index selection techniques (QPQ-NN and QPQ-MC)]

Class	Metric	PRMS	DAR-NN	QPQ-NN	DAR-MC	QPQ-MC
Overall goodness of fit	Nash-Sutcliffe efficiency of streamflows	2.64	2.64	2.70	3.02	3.23
	Nash-Sutcliffe efficiency of the logarithms of streamflow	4.98	1.95	2.09	2.66	2.55
	Root-mean-squared error of streamflow	2.64	2.64	2.70	3.02	3.23
	Root-mean-square-normalized error of streamflow	4.91	2.18	1.80	2.82	2.52
	Average percent error of streamflow	4.64	2.59	2.05	2.84	2.11
	Pearson correlation between observed and simulated streamflow	2.93	2.55	2.73	2.89	3.14
	Spearman correlation between observed and simulated streamflow	5.00	1.50	2.23	2.27	3.16
	Average	3.96	2.29	2.33	2.79	2.85
	Standard deviation	1.16	0.44	0.38	0.26	0.45
	Storage-yield curve (SYC) goodness of fit	Nash-Sutcliffe efficiency of required storage	4.41	2.27	2.39	2.68
Nash-Sutcliffe efficiency of the logarithms of required storage		4.57	2.34	2.20	2.86	2.18
Root-mean-squared error of required storage		4.41	2.27	2.39	2.68	2.48
Root-mean-square-normalized error of required storage		4.73	2.48	2.11	2.84	2.07
Average percent error of required storage		4.70	2.45	2.07	2.89	2.11
Pearson correlation between observed and simulated required storage		4.32	2.09	2.34	2.50	2.98
Spearman correlation between observed and simulated required storage		1.55	1.00	1.05	1.50	1.09
Average		4.10	2.13	2.08	2.50	2.20
Standard deviation		1.14	0.51	0.47	0.66	0.58
Percent error in streamflow statistics		Root-mean-square-normalized error of fundamental daily streamflow statistics	4.09	2.57	2.07	3.25
	Coefficient of variation of annual streamflow	3.86	2.50	2.39	2.61	2.86
	Coefficient of variation of daily streamflow	3.48	2.82	2.52	3.05	2.36
	10th percentile, 7-day average annual-minimum streamflow	3.86	2.82	2.09	3.30	2.11
	50th percentile, 7-day average annual-minimum streamflow	4.43	2.75	2.02	2.98	2.02
	90th percentile, annual-maximum streamflow	2.89	3.14	2.25	3.64	2.27
	90-percent-exceedance streamflow	3.89	2.84	2.39	2.93	2.14
	75-percent-exceedance streamflow	3.82	2.59	2.36	3.14	2.30
	50-percent-exceedance streamflow	3.68	2.27	2.80	2.64	2.80
	25-percent-exceedance streamflow	3.32	2.23	2.98	2.64	3.00
Mean streamflow	10-percent-exceedance streamflow	3.64	2.43	2.68	2.77	2.68
	Mean streamflow	2.66	2.32	3.18	2.77	3.30
	L-CV of daily streamflow	3.70	2.86	2.34	3.09	2.23
	L-skewness of daily streamflow	4.16	2.45	2.16	3.25	2.20
	L-kurtosis of daily streamflow	3.82	2.34	2.36	3.18	2.52
	Lag-1 autocorrelation of daily streamflow	1.93	2.93	2.93	3.23	3.20
	Amplitude of seasonal trend in daily streamflow	3.07	2.75	2.43	3.41	2.57
	Phase of seasonal trend in daily streamflow	4.57	1.84	2.64	2.34	2.84
	Average	3.60	2.58	2.48	3.01	2.54
	Standard deviation	0.65	0.32	0.33	0.33	0.39
All metrics	Average	3.79	2.42	2.36	2.85	2.53
	Standard deviation	0.89	0.42	0.40	0.45	0.48

logarithmic NSE of the daily, no-fail storage-yield curve and with regard to the coefficient of variation of streamflows and low-flow metrics including the 10th and 25th percentiles of daily streamflow. Previously, Farmer and others (2014) found a much larger difference between the two methods for the selection of index streamgages, but, for this study, the slight advantage of the NN method is consistent with their findings. For the majority of the performance metrics, QPPQ-NN is ranked more favorably than DAR-NN. However, DAR-NN yielded a better average ranking with the NSE, NSEL, RMSE and correlations of streamflow. Additionally, DAR-NN more accurately estimated the higher percentiles of daily streamflow, while QPPQ-NN was better at reproducing the variability of streamflow and the low-flow behavior.

The PRMS shows a consistently poor ranking across almost all metrics, indicating that the process-based approach does not perform as well in this region. This finding is again consistent with the findings of Farmer and others (2014). The PRMS does provide a strong ranking with respect to the NSE and RMSE of streamflows. Since the PRMS was calibrated at reference sites using the NSE, this strong ranking is not surprising. More interesting is the superiority of the PRMS in reproducing the lag-one correlation of streamflow. This provides evidence that the mechanistic, process-based structure of the PRMS is accurately reproducing the at-site lag behavior. The transfer-based methods may not be reproducing the at-site lag behavior as well because they rely on the lag structure of an index streamgage alone.

The standard deviations of the ranks of each PUB method according to each performance metric (table 3) indicate the consistency of the performance for each PUB metric. Across all the metrics, the PRMS and DAR-MC show the most variability. For some metrics, like RMSNE and average percent error of streamflow, the PRMS is the least variable. However, the QPPQ methods show the least variability when averaged across all metrics, and, coupled with the average performance presented earlier, QPPQ-NN shows the most consistent (least-variable) accuracy.

The information in tables 2 and 3 is summarized in an RRBE cloud with variability ellipses in figure 3. QPPQ-NN demonstrates the best and most consistent performance out of these five methods. The point representing QPPQ-NN is on the optimal edge of the RRBE cloud, having the best average ranking and the smallest average standard deviation. DAR-NN has slightly more variability with an increased average rank. QPPQ-NN also has the smallest variability ellipse. QPPQ-MC shows a more flattened ellipse, demonstrating that QPPQ-MC has a more consistent amount of variability with a greater variability in the mean across metrics. The ellipses demonstrate the substantial overlap between the methods. The substantial overlap between QPPQ-NN and QPPQ-MC shows that the QPPQ method is not overly sensitive to the index-selection algorithm. The smaller overlap between DAR-NN and DAR-MC shows that DAR is more sensitive to the index-selection algorithm.

Finally, DAR-NN and QPPQ-NN, the two best methods, show a high degree of overlap. While QPPQ-NN appears to be better overall, DAR-NN may be more appropriate in some situations. The transfer-based methods are strongest and have similarly-sized variability ellipses, but the PRMS is set back much further and has a large variability ellipse.

The threshold analysis in figure 4 again shows that the transfer-based methods are superior to the ungaged mechanistic model. The curves represent the mean, across sites, percent of the validation record that has an absolute percent error below the error threshold. For all error thresholds, the transfer-based methods have a greater portion of the validation record below the threshold. The curves of the transfer-based methods rise more quickly and begin to level out at a higher proportion than the PRMS. For the transfer-based methods, nearly 50 percent of the validation record is less than the 25 percent error threshold, compared to only 26 percent of the validation record for the PRMS. At an error threshold of 100 percent of the observations, more than 90 percent of the validation record is less than the threshold for transfer-based methods; only 75 percent for the PRMS. The transfer-based methods are clustered quite closely, but QPPQ-NN is on the leading edge. For the validation record, 90 percent of the QPPQ-NN predictions, on average, are less than the 80 percent threshold. As these are just averages, figure 5 characterizes the variability of each PUB method at each threshold by displaying the coefficient of variation of the percentage of the validation record less than the error threshold across sites. The variability decreases for higher thresholds and the PRMS shows a greater variability than the transfer-based methods.

The transfer-based methods are able to reproduce daily streamflow records more accurately than the ungaged application of the PRMS, a mechanistic model. This result agrees with the findings of Farmer and others (2014) in the southeastern United States. Linhart and others (2013), in contrast, showed that a fully-calibrated, at-site application of process-based models, a technique that could not be applied at ungaged locations, out-performed regionally-calibrated, transfer-based methods in the same region as this study. Linhart and others (2013) considered both QPPQ and the Flow-Anywhere (FA) method, a calibrated version of the DAR method, but did not consider a validation framework. Linhart and others (2012) demonstrated that their at-site calibration of PRMS showed a greater NSE than the transfer-based methods. From Linhart and others (2013), PRMS had a median NSE of 0.66, while FA and QPPQ had medians of 0.37 and 0.55, respectively. Though a larger and different set of sites was used in this report, the PRMS had a median of 0.69, while DAR-NN and QPPQ-NN yielded NSE values of 0.65 and 0.67, respectively. The relative comparison is the same, but the results in table 2 show that the consideration of additional metrics, an analysis which Linhart and others (2013) call for, does not favor the performance of the PRMS. This suggests that the model structure of the PRMS is sufficient for reproducing fairly accurate, independent, day-to-day predictions, but, when run in an ungaged

Table 3. Standard deviation of the ranks for each performance metric and method of prediction in ungaged basins (PUB).

[At each site, the PUB methods were ranked according to a single metric, with the best method receiving the lowest rank. These standard deviations were taken across 44 sites for each PUB method. The process was repeated for each of the 32 metrics and 5 PUB methods. The PUB methods include the Precipitation Runoff Modeling System (PRMS), drainage-area ratio with the nearest-neighboring index streamgage (DAR-NN) or the map-correlated index streamgage (DAR-MC) and nonlinear spatial interpolation using flow duration curves with the same index selection techniques (QPPQ-NN and QPPQ-MC)]

Class	Metric	PRMS	DAR-NN	QPPQ-NN	DAR-MC	QPPQ-MC	
Overall goodness of fit	Nash-Sutcliffe efficiency of streamflows	1.66	1.24	1.32	1.39	1.29	
	Nash-Sutcliffe efficiency of the logarithms of streamflow	0.15	1.14	0.88	1.27	1.00	
	Root-mean-squared error of streamflow	1.66	1.24	1.32	1.39	1.29	
	Root-mean-square-normalized error of streamflow	0.60	0.99	1.07	1.17	1.00	
	Average percent error of streamflow	0.94	1.19	1.01	1.35	1.04	
	Pearson correlation between observed and simulated streamflow	1.70	1.32	1.23	1.45	1.27	
	Spearman correlation between observed and simulated streamflow	0.00	0.85	0.89	1.11	0.91	
	Average	0.96	1.14	1.10	1.30	1.11	
	Standard deviation	0.73	0.16	0.19	0.13	0.16	
	Storage-yield curve (SYC) goodness of fit	Nash-Sutcliffe efficiency of required storage	1.19	1.21	1.10	1.39	1.19
		Nash-Sutcliffe efficiency of the logarithms of required storage	0.76	1.22	1.07	1.39	1.13
Root-mean-squared error of required storage		1.19	1.21	1.10	1.39	1.19	
Root-mean-square-normalized error of required storage		0.54	1.28	0.99	1.31	1.11	
Average percent error of required storage		0.59	1.27	1.04	1.28	1.13	
Pearson correlation between observed and simulated required storage		1.27	1.20	1.16	1.27	1.19	
Spearman correlation between observed and simulated required storage		1.32	0.00	0.30	0.30	0.42	
Average		0.98	1.05	0.97	1.19	1.05	
Standard deviation		0.34	0.47	0.30	0.40	0.28	
Percent error in streamflow statistics		Root-mean-square-normalized error of fundamental daily streamflow statistics	1.44	1.25	0.93	1.38	1.12
		Coefficient of variation of annual streamflow	1.59	1.27	1.32	1.33	1.19
	Coefficient of variation of daily streamflow	1.55	1.45	1.09	1.63	1.10	
	10th percentile, 7-day average annual-minimum streamflow	1.46	1.28	0.96	1.44	1.10	
	50th percentile, 7-day average annual-minimum streamflow	1.13	1.26	1.13	1.28	0.93	
	90th percentile, annual-maximum streamflow	1.56	1.19	1.20	1.30	1.32	
	90-percent-exceedance streamflow	1.51	1.36	1.26	1.40	1.07	
	75-percent-exceedance streamflow	1.48	1.39	1.26	1.39	1.09	
	50-percent-exceedance streamflow	1.68	1.30	1.11	1.46	1.15	
	25-percent-exceedance streamflow	1.60	1.27	1.27	1.40	1.28	
	10-percent-exceedance streamflow	1.64	1.30	1.25	1.43	1.23	
	Mean streamflow	1.45	1.25	1.37	1.46	1.34	
	L-CV of daily streamflow	1.55	1.32	1.12	1.60	1.08	
	L-skewness of daily streamflow	1.22	1.25	1.10	1.30	1.21	
	L-kurtosis of daily streamflow	1.35	1.36	1.14	1.51	1.19	
	Lag-1 autocorrelation of daily streamflow	1.35	1.30	1.30	1.33	1.21	
	Amplitude of seasonal trend in daily streamflow	1.70	1.48	1.00	1.42	1.13	
	Phase of seasonal trend in daily streamflow	1.19	0.94	1.08	1.18	1.20	
	Average	1.47	1.29	1.16	1.40	1.16	
Standard deviation	0.17	0.11	0.13	0.11	0.10		
All metrics	Average	1.25	1.21	1.11	1.33	1.13	
	Standard deviation	0.45	0.25	0.20	0.22	0.17	

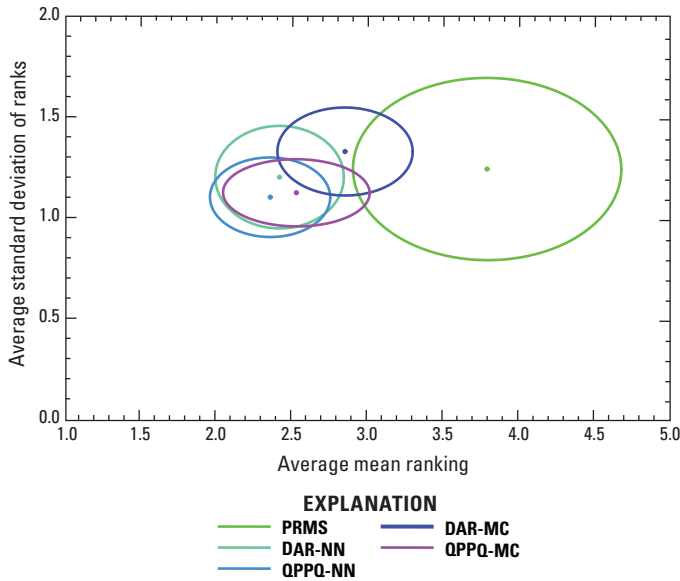


Figure 3. Robust rank-based evaluation cloud showing the tradeoff between the mean ranking and standard deviation of the ranks of the 32 performance metrics for each method of prediction in ungaged basins. See text for a description of each performance metric. Horizontal axis shows the mean average rank, while the vertical axis gives the average standard deviation of the ranks. Optimal methods would display minimal spread and a low mean-average ranking. Variability ellipses indicate the spread across the 32 metrics for each prediction method. The PUB methods include the Precipitation Runoff Modeling System (PRMS), drainage-area ratio with the nearest-neighboring index streamgage (DAR-NN) or the map-correlated index streamgage (DAR-MC), and nonlinear spatial interpolation using flow duration curves with the same index selection techniques (QPPQ-NN and QPPQ-MC)]

mode, the PRMS is unable to reproduce the statistical and distributional properties of the historical record. Linhart and others (2013) noted that the PRMS was limited by the region of calibration and Farmer and others (2014) postulated that a more robust method of ungaged calibration could improve the performance of the PRMS.

Of the transfer-based methods, QPPQ-NN produces a predicted record that most accurately reproduces the statistical and distributional properties of historical record on average. Linhart and others (2012) also showed that, in Iowa, QPPQ performed better than the FA method, a method quite similar to the DAR method. When applied by Linhart and others (2012) in a study that did not consider the PRMS, FA had a median NSE of 0.66 and QPPQ had a median of 0.73. As is affirmed by the findings here, the comparison NSELs was much tighter: Linhart and others (2012) showed FA to have a median NSEL of 0.76 (DAR-NN had a median of 0.86 in this report) and QPPQ had a median of 0.80 (QPPQ-NN had a median of 0.87 in this report). The results of Linhart and others (2013), when the process-based models are left aside, also show that QPPQ is preferred over FA. These relative

comparisons of NSE and NSEL, among many metrics, also agree with the results of Farmer and others (2014). Though Farmer and others (2014) considered a wider range of transfer-based methods, QPPQ-NN out-performed the other methods, on average.

While QPPQ-NN was shown to be the best PUB method considered on average, it still has some limitations. Linhart and others (2013) noted that the relative performance of PUB methods may vary across flow regimes, from high flows to low flows. Farmer and others (2014) make a similar observation, looking across performance metrics. QPPQ-NN may be the best PUB method on average, but may not be the best for particular applications. For example, the PRMS is able to more accurately reproduce the lag behavior, even if QPPQ-NN is superior in many other ways. It is therefore useful to consider the intended application before selecting a PUB method. In addition, the three-step nature of transfer methods (index selection, regression parameterization and transfer between index and ungaged location) like QPPQ opens several ingresses for model uncertainty (Linhart and others, 2012; Farmer and Vogel, 2013). With these multiple uncertainties it is difficult to state the confidence in any one prediction or identify the areas for improvement. A better understanding of the error structure of ungaged predictions may improve the application of PUB methods.

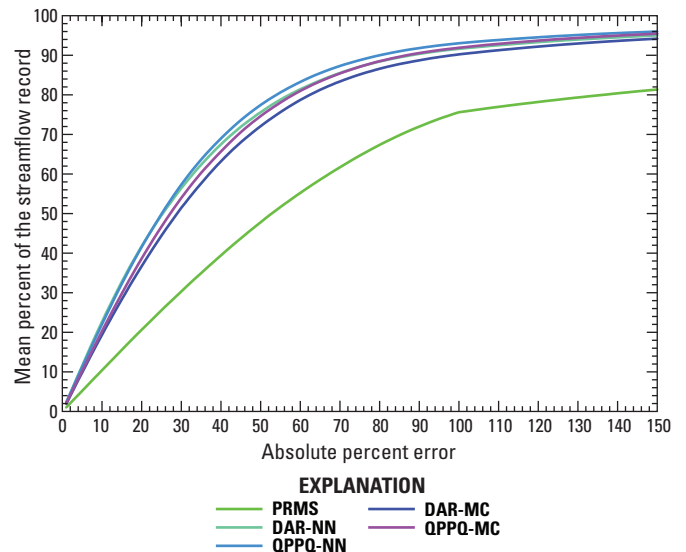


Figure 4. For all methods of prediction in ungaged basins, the cross-site mean fraction of the validation record less than a threshold absolute percent error, a cumulative distribution of the absolute percent error, is presented here. The horizontal axis indicates the absolute percent error threshold and the vertical axis indicated the percent of predictions less than the corresponding threshold. The PUB methods include the Precipitation Runoff Modeling System (PRMS), drainage-area ratio with the nearest-neighboring index streamgage (DAR-NN) or the map-correlated index streamgage (DAR-MC), and nonlinear spatial interpolation using flow duration curves with the same index selection techniques (QPPQ-NN and QPPQ-MC).

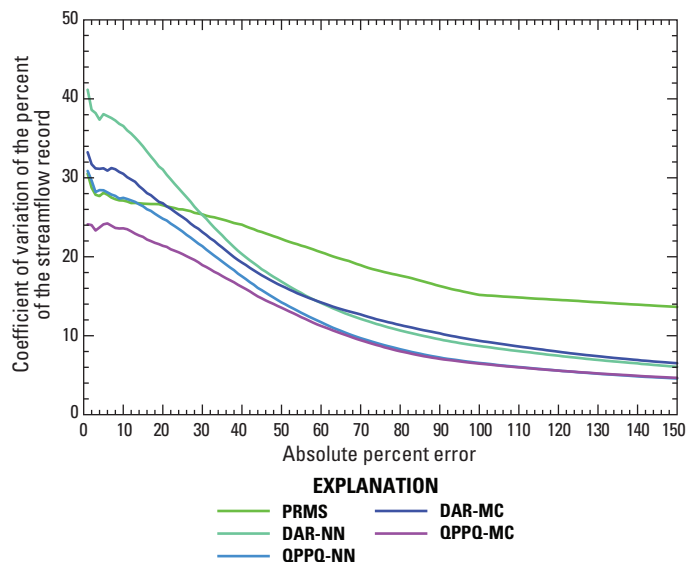


Figure 5. For all methods of prediction in ungaged basins, the cross-site coefficient of variation of the fraction of the validation record less than a threshold absolute percent error is presented here. The horizontal axis indicates the absolute percent error threshold and the vertical axis indicates the cross-site coefficient of variation of the fraction of the validation record less than the corresponding threshold. The PUB methods include the Precipitation Runoff Modeling System (PRMS), drainage-area ratio with the nearest-neighboring index streamgauge (DAR-NN) or the map-correlated index streamgauge (DAR-MC), and nonlinear spatial interpolation using flow duration curves with the same index selection techniques (QPPQ-NN and QPPQ-MC).

Summary and Conclusions

Records of daily streamflow are essential to water resources management and planning as well as hydrologic understanding. Many regions of the world, even in the United States, remain sparsely gaged. The U.S. Geological Survey's National Water Census has sought to fill those gaps using various tools for prediction in ungaged basins. Building on previous research in Iowa and the southeastern United States, this report documents the comparison of several methods for prediction of ungaged basins, including nearest-neighbor and map-correlation applications of drainage area ratios and nonlinear spatial interpolation using flow duration curves, along with an ungaged application of the Precipitation-Runoff Modeling System. In contrast to the southeastern United States, the Des Moines and Iowa Rivers in Iowa are characterized by a different hydroclimatic regime, less variation in elevation, and a variety of different landform regions.

Using five methods for prediction in ungaged basins, streamflow records were reproduced in a threefold validation across 44 watersheds in the Des Moines and Iowa River Basins. The drainage area ratio technique requires no calibration, but is similar to other "Flow Anywhere" techniques.

Nonlinear spatial interpolation using flow duration curves was applied using regional-regression estimated flow duration curves at ungaged locations. Each of these statistical techniques was implemented with a nearest-neighbor index streamgauge based on spatial proximity and a map-correlated index streamgauge based on estimated hydrograph correlation. The Precipitation-Runoff Modeling System was run in an ungaged mode to produce a mechanistic, process-based estimate of ungaged streamflow.

The methods for prediction in ungaged basins were analyzed using the Robust Rank-Based Evaluation and an assessment of the cumulative distribution of the daily percent errors. Averaging across all performance metrics, the nearest-neighbor implementation of the nonlinear spatial interpolation using flow duration curves showed the best ability to reproduce the statistical and distributional properties of the historical record. This agrees with previous work in the region and similar studies in other regions. The transfer-based methods were shown to be generally superior to the ungaged application of the process-based Precipitation-Runoff Modeling System. Considering a restricted set of performance metrics in the Cedar River Basin, calibrated iterations of the PRMS have previously been shown to out-perform transfer-based methods. The broader set of performance metric shown in this report, however, highlights the weaknesses of an ungaged calibration of the Precipitation Runoff Modeling System.

Additional research may improve the performance of prediction in ungaged basins. Prediction of historical records can continue to be improved by considering additional study regions in which to assess prediction in ungaged basins. In particular, an arid or a snow-dominated region may provide additional information not gathered from this analysis or previous work done in the southeastern United States. Furthermore, understanding the uncertainty of streamflow predictions could further refine prediction in ungaged basins and inform the use of predictions in water management decisions and planning. Such research might show that predictions for specific flow regimes may be improved using specific prediction methods. Continuing to explore regional studies of prediction in ungaged basins will surely improve national and international implementations and lead to more informed and responsible use and management of water resources.

Acknowledgments

This report was produced as a part of the USGS National Water Census and also supports the goals of the National Streamflow Information Program.

We offer our special thanks to Sara Levin and Parker Norton (USGS) who provided exceptional reviews of the original manuscript and vastly improved the final product.

References Cited

- Alley, W.M., Evenson, E.J., Barber, N.L., Bruce, B.W., Dennehy, K.F., Freeman, M.C., Freeman, W.O., Fischer, J.M., Hughes, W.B., Kennen, J.G., Kiang, J.E., Maloney, K.O., Musgrove, M., Ralston, B., Tessler, S., and Verdin, J.P., 2013, Progress toward establishing a national assessment of water availability and use: U.S. Geological Survey Circular 1384, 34 p., available at <http://pubs.usgs.gov/circ/1384/>.
- Archfield, S.A., and Vogel, R.M., 2010, Map correlation method: Selection of a reference streamgage to estimate daily streamflow at ungauged catchments: *Water Resources Research*, v. 46, no. 10, available at <http://dx.doi.org/10.1029/2009WR008481>.
- Archfield, S.A., Kennen, J.G., Carlisle, D.M., and Wolock, D.M., 2013, An objective and Parsimonious approach for classifying natural flow regimes at a continental scale: *River Research and Applications*, v. 30, no. 9, p. 1166–1183, available at <http://dx.doi.org/10.1002/rra.2710>.
- Asquith, W.H., Roussel, M.C., and Vrabel, J., 2006, Statewide analysis of the drainage-area ratio method for 34 streamflow percentile ranges in Texas: U.S. Geological Survey Scientific Investigations Report 2006–5286, 34 p., available at <http://pubs.usgs.gov/sir/2006/5286/>.
- Duan, Q.Y., Gupta, V.K., and Sorooshian, S., 1993, Shuffled complex evolution approach for effective and efficient global minimization: *Journal of Optimization Theory and Applications*, v. 76, no. 3, p. 501–521.
- Duan, Q.Y., Sorooshian, S., and Gupta, V.K., 1992, Effective and efficient global optimization for conceptual rainfall-runoff models: *Water Resources Research*, v. 28, no. 4, p. 1015–1031.
- Duan, Q.Y., Sorooshian, S., and Gupta, V.K., 1994, Optimal use of the SCE-UA global optimization method for calibrating watershed models: *Journal of Hydrology*, v. 158, no. 3–4, p. 265–284.
- Eash, D.A., 2001, Techniques for estimating flood-frequency discharges for streams in Iowa: U.S. Geological Survey Water-Resources Investigations Report 2000–0423, 88 p., available at http://ia.water.usgs.gov/pubs/reports/WRIR_2000-4233.pdf.
- Eash, D.A., Barnes, K.K., and Veilleux, A.G., 2013, Methods for estimating annual exceedance-probability discharges for streams in Iowa, based on data through water year 2010: U.S. Geological Survey Scientific Investigations Report 2013–5086, 63 p. with appendix, available at <http://pubs.usgs.gov/sir/2013/5086/>.
- Eng, K., and Milly, P.C.D., 2007, Relating low-flow characteristics to the base flow recession time constant at partial record stream gauges, *Water Resources Research*, v. 43, available at <http://dx.doi.org/10.1029/2006WR005293>.
- Falcone, J.A., 2011, GAGES-II: Geospatial Attributes of Gages for Evaluating Streamflow: U.S. Geological Survey digital spatial dataset, available at http://water.usgs.gov/GIS/metadata/usgswrd/XML/gagesII_Sept2011.xml.
- Farmer, W.H., 2015, Estimating records of daily streamflow at ungauged location in the southeast United States: Medford, Mass., Tufts University, Ph.D. dissertation, 416 p.
- Farmer, W.H., and Vogel, R.M., 2013, Performance-weighted methods for estimating monthly streamflow at ungauged sites: *Journal of Hydrology*, v. 477, p. 240–250, available at <http://dx.doi.org/10.1016/j.jhydrol.2012.11.032>.
- Farmer, W.H., Archfield, S.A., Over, T.M., Hay, L.E., LaFontaine, J.H., and Kiang, J.E., 2014, A comparison of methods to predict historical daily streamflow time series in the southeastern United States: U.S. Geological Survey Scientific Investigations Report 2014–5231, 34 p., <http://dx.doi.org/10.3133/sir20145231>.
- Fennessey, N.M., 1994, A hydro-climatological model of daily stream flow for the northeast United States: Medford, Mass., Tufts University, Ph.D. dissertation, 269 p.
- Hirsch, R.M., 1979, An evaluation of some record reconstruction techniques: *Water Resources Research*, v. 15, no. 6, p. 1781–1790, available at <http://dx.doi.org/10.1029/wr015i006p01781>.
- Homer, C., Huang, C., Yang, L., Wylie, B., Coan, M., 2004, Development of a 2001 national land-cover database for the United States: *Photogrammetric Engineering and Remote Sensing*, v. 70, no. 7, p. 829–840, available at <http://www.asprs.org/a/publications/pers/2007journal/april/highlight.pdf>.
- Hrachowitz, M., Savenije, H.H.G., Bloschl, G., McDonnell, J.J., Sivapalan, M., Pomeroy, J.W., Arheimer, B., Blume, T., Clark, M.P., Ehret, U., Fenicia, F., Freer, J.E., Gelfan, A., Gupta, H.V., Hughes, D.A., Hut, R.W., Montanari, A., Pande, S., Tetzlaff, D., Troch, P.A., Uhlenbrook, S., Wagener, T., Winsemius, H.C., Woods, R.A., Zehe, E., and Cudennec, C., 2013, A decade of Predictions in Ungauged Basins (PUB)—A review: *Hydrological Sciences Journal*, v. 58, no. 6, p. 1198–1255, available at <http://dx.doi.org/10.1080/02626667.2013.803183>.
- Huff, F.A., and Angel, J.R., 1992, Rainfall frequency atlas of the midwest: *Illinois State Water Survey Bulletin*, v. 71, 141 p., available at <http://www.isws.illinois.edu/pubdoc/B/ISWSB-71.pdf>.
- Hughes, D.A., and Smakhtin, V., 1996, Daily flow time series patching or extension: A spatial interpolation approach based on flow duration curves: *Hydrologic Sciences Journal*, v. 41, no. 6, p. 851–871.
- Iowa Department of Natural Resources, 2006, Total maximum daily load for nitrate, Cedar River, Linn County, Iowa, 2006: Iowa Department of Natural Resources, Des Moines, Iowa, 62 p., available at http://www.epa.gov/waters/tmdl/docs/32009_IACedarRiverTMDL.pdf.
- Kiang, J.E., Stewart, D.W., Archfield, S.A., Osborne, E.B., and Eng, K., 2013, A national streamflow network gap analysis: U.S. Geological Survey Scientific Investigations Report 2013–5013, 79 p., available at <http://pubs.er.usgs.gov/publication/sir20135013>.

- Koltun, G.F., and Whitehead, M.T., 2002, Techniques for estimating selected streamflow characteristics of rural, unregulated streams in Ohio: U.S. Geological Survey Water-Resources Investigations Report 2002–4068, 50 p., available at <http://oh.water.usgs.gov/reports/wrir/wrir02-4068.pdf>.
- Larimer, O.J., 1957, Drainage areas of Iowa streams: Iowa Research Board Bulletin No. 7, 439 p. (Reprinted 1974).
- Leavesley, G.H., Lichty, R.W., Troutman, B.M., and Saindon, L.G., 1983, Precipitation-runoff modeling system: User's manual: U.S. Geological Survey Water-Resources Investigations Report 83–4238, 207 p., available at <http://pubs.er.usgs.gov/publication/wri834238>.
- Linhart, S.M., Nania, J.F., Sanders, Jr., C.L., and Archfield, S.A., 2012, Computing daily mean streamflow at ungauged locations in Iowa by using the Flow Anywhere and Flow Duration Curve Transfer statistical methods: U.S. Geological Survey Scientific Investigations Report 2012–5232, 50 p., available at <http://pubs.er.usgs.gov/publication/sir20125232>.
- Linhart, S.M., Nania, J.F., Christiansen, D.E., Hutchinson, K.J., Sanders, Jr., C.L., and Archfield, S.A., 2013, Comparison between two statistically based methods, and two physically based models developed to compute daily mean streamflow at ungauged locations in the Cedar River Basin, Iowa: U.S. Geological Survey Scientific Investigations Report 2013–5111, 7 p., available at <http://pubs.er.usgs.gov/publication/sir20135111>.
- Markstrom, S.L., Niswonger, R.G., Regan, R.S., Prudic, D.E., and Barlow, P.M., 2008, GSFLOW—Coupled ground-water and surface-water flow model based on the integration of the Precipitation-Runoff Modeling System (PRMS) and the Modular Ground-Water Flow Model (MODFLOW-2005): U.S. Geological Survey Techniques and Methods, book 6, chap. D–1, 240 p., available at <http://pubs.er.usgs.gov/publication/tm6D1>.
- Markstrom, S.L., Regan, R.S., Hay, L.E., Viger, R.J., Webb, R.M.T., Payn, R.A., and LaFontaine, J.H., 2014, PRMS-IV, the precipitation-runoff modeling system, version 4: U.S. Geological Survey Techniques and Methods, book 6, chap. B7, 158 p., available at <http://dx.doi.org/10.3133/tm6B7>.
- Mohamoud, Y.M., 2008, Prediction of daily flow duration curves and streamflow for ungauged catchments using regional flow duration curves: *Hydrological Sciences Journal*, v. 53, no. 4, p. 706–724, available at <http://dx.doi.org/10.1623/hysj.53.4.706>.
- Nash, J.E., and Sutcliffe, J.V., 1970, River flow forecasting through conceptual models part I—A discussion of principles: *Journal of Hydrology*, v. 10, no. 3, p. 282–290, available at [http://dx.doi.org/10.1016/0022-1694\(70\)90255-6](http://dx.doi.org/10.1016/0022-1694(70)90255-6).
- Prior, J.C., Kohrt, C.J., and Quade, D.J., 2009, The landform regions of Iowa: Iowa City, Iowa, Iowa Geological Survey, Iowa Department of Natural Resources, vector digital data, accessed December 15, 2011, available at <http://www.igsb.uiowa.edu/webapps/nrgislibx/>.
- Salazar, Ken, 2010, Secretarial Order 3297, Department of the Interior WaterSMART program—Sustain and manage America's resources for tomorrow: U.S. Department of the Interior, 4 p.
- Shu, C., and Ouarda, T.B.M.J., 2012, Improved methods for daily streamflow estimates at ungauged sites: *Water Resources Research*, v. 48, no. 2, available at <http://dx.doi.org/10.1029/2011WR011501>.
- Sivapalan, Murugesu, 2003, Prediction in ungauged basins: A grand challenge for theoretical hydrology: *Hydrological Processes*, v.17, no. 15, p. 3163–3170, available at <http://dx.doi.org/10.1002/hyp.5155>.
- Sivapalan, Murugesu, Takeuchi, K., Franks, S.W., Gupta, V.K., Karambiri, H., Lakshmi, V., Liang, X., McDonnell, J.J., Mendiondo, E.M., O'Connell, P.E., Oki, T., Pomeroy, J.W., Schertzer, D., Uhlenbrook, S., and Zehe, E., 2003, IAHS decade on Predictions in Ungauged Basins (PUB), 2003–2012: Shaping an exciting future for the hydrological sciences: *Hydrological Sciences Journal*, v. 48, no. 6, p. 857–880, available at <http://dx.doi.org/10.1623/hysj.48.6.857.51421>.
- Smakhtin, V.Y., 1999, Generation of natural daily flow time-series in regulated rivers using a non-linear spatial interpolation technique: *River Research and Applications*, v. 15, no. 4, p. 311–323, available at [http://dx.doi.org/10.1002/\(SICI\)1099-1646\(199907/08\)15:4<311::AID-RRR544>3.0.CO;2-W](http://dx.doi.org/10.1002/(SICI)1099-1646(199907/08)15:4<311::AID-RRR544>3.0.CO;2-W).
- Stedinger, J.R., Vogel, R.M., and Foufoula-Georgiou, E., 1993, Frequency analysis of extreme events, *in* Maidment, D.R., ed., *Handbook of hydrology*: New York, McGraw-Hill, variously paged.
- U.S. Geological Survey, 2007, Facing tomorrow's challenges—U.S. Geological Survey science in the decade 2007–2017: U.S. Geological Survey Circular 1309, × + 70 p.
- Viglione, A., Parajka, J., Rogger, M., Salinas, J.L., Laaha, G., Sivapalan, M., and Blöschl, G., 2013, Comparative assessment of predictions in ungauged basins—Part 3: Runoff signatures in Austria: *Hydrology and Earth System Sciences*, v. 17, no. 6, p. 2263–2279, available at <http://dx.doi.org/10.5194/hess-17-2263-2013>.
- Vogel, R.M., 2011, Hydromorphology: *Journal of Water Resources Planning and Management*, v. 137, no. 2, p. 147–149, available at [http://dx.doi.org/10.1061/\(ASCE\)WR.1943-5452.0000122](http://dx.doi.org/10.1061/(ASCE)WR.1943-5452.0000122).
- Wahl, K.L., and Wahl, T.L., 1988, Effects of regional ground-water declines on streamflows in the Oklahoma Panhandle, *in* Proceedings of Symposium on Water-Use Data for Water Resources Management: Tucson, Arizona, American Water Resources Association, p. 239–249, available at http://www.usbr.gov/pmts/hydraulics_lab/twahl/bfi/bfi_beaver_river.pdf.

Appendix 1. Stations Used in Analysis

Appendix 1. Names, station numbers, fraction of zeros, and period of record for each streamgage used for the comparison of methods of prediction in ungaged basins in the Des Moines and Iowa River Basins.

[Water year is defined as a continuous period from October 1 through September 30]

Station number	Station name (index number on figure 2)	Validation set	Latitude (decimal degrees)	Longitude (decimal degrees)	Drainage area (square miles)	Mean streamflow (cubic feet per second)	Zero-flow days (Percent of record)	Number of complete water years	First water year	Last water year
05449500	Iowa River near Rowan (1)	3	42.76	-93.62	429.0	339.5	0.00	29	1982	2011
05451210	South Fork Iowa River NE of New Providence (2)	1	42.32	-93.15	224.0	195.1	0.00	15	1996	2011
05451500	Iowa River at Marshalltown (3)	2	42.07	-92.91	1,532.0	1,286.6	0.00	29	1982	2011
05451700	Timber Creek near Marshalltown (4)	3	42.01	-92.85	118.0	110.3	0.00	29	1982	2011
05451900	Richland Creek near Haven (5)	1	41.90	-92.47	56.1	49.9	0.02	29	1982	2011
05452000	Salt Creek near Elberon (6)	3	41.96	-92.31	201.0	175.1	0.00	29	1982	2011
05452200	Walnut Creek near Hartwick (7)	1	41.84	-92.39	70.9	61.7	0.00	29	1982	2011
05453000	Big Bear Creek at Ladora (8)	2	41.75	-92.18	189.0	165.5	0.00	29	1982	2011
05453100	Iowa River at Marengo (9)	1	41.81	-92.06	2,794.0	2,424.1	0.00	29	1982	2011
05454000	Rapid Creek near Iowa City (10)	1	41.70	-91.49	25.3	20.9	2.62	29	1982	2011
05454220	Clear Creek near Oxford (11)	3	41.72	-91.74	58.4	51.3	0.00	17	1994	2011
05454300	Clear Creek near Coralville (12)	1	41.68	-91.60	98.1	86.1	0.00	29	1982	2011
05455100	Old Mans Creek near Iowa City (13)	1	41.61	-91.62	201.0	167.2	0.00	27	1984	2011
05455500	English River at Kalona (14)	3	41.47	-91.71	574.0	484.8	0.00	29	1982	2011
05457000	Cedar River near Austin, Minnesota (15)	1	43.64	-92.97	399.0	347.3	0.00	29	1982	2011
05457700	Cedar River at Charles City (16)	3	43.06	-92.67	1,054.0	884.2	0.00	25	1982	2011
05458000	Little Cedar River near Ionia (17)	2	43.03	-92.50	306.0	229.7	0.00	29	1982	2011
05458500	Cedar River at Janesville (18)	3	42.65	-92.47	1,661.0	1,411.7	0.00	29	1982	2011
05458900	West Fork Cedar River at Finchford (19)	2	42.63	-92.54	846.0	760.2	0.00	29	1982	2011
05459500	Winnebago River at Mason City (20)	2	43.16	-93.19	526.0	403.6	0.00	29	1982	2011
05462000	Shell Rock River at Shell Rock (21)	3	42.71	-92.58	1,746.0	1,370.0	0.00	29	1982	2011
05463000	Beaver Creek at New Hartford (22)	3	42.57	-92.62	347.0	318.3	0.00	29	1982	2011
05463500	Black Hawk Creek at Hudson (23)	2	42.41	-92.46	303.0	277.2	0.00	23	1982	2011
05464000	Cedar River at Waterloo (24)	3	42.50	-92.33	5,146.0	4,458.3	0.00	29	1982	2011
05464220	Wolf Creek near Dysart (25)	2	42.25	-92.30	299.0	275.2	0.00	12	1996	2011
05464500	Cedar River at Cedar Rapids (26)	1	41.97	-91.67	6,510.0	5,696.8	0.00	29	1982	2011
05465000	Cedar River near Conesville (27)	2	41.41	-91.29	7,787.0	6,890.1	0.00	29	1982	2011
05476750	Des Moines River at Humboldt (28)	1	42.72	-94.22	2,256.0	1,415.8	0.00	29	1982	2011
05479000	East Fork Des Moines River at Dakota City (29)	1	42.72	-94.19	1,308.0	902.8	0.00	29	1982	2011
05480500	Des Moines River at Fort Dodge (30)	2	42.51	-94.20	4,190.0	2,765.5	0.00	29	1982	2011
05481000	Boone River near Webster City (31)	3	42.43	-93.81	844.0	688.5	0.00	29	1982	2011
05481300	Des Moines River near Stratford (32)	2	42.25	-94.00	5,452.0	3,745.5	0.00	29	1982	2011
05481950	Beaver Creek near Grimes (33)	3	41.69	-93.74	358.0	265.3	0.00	29	1982	2011
05482300	North Raccoon River near Sac City (34)	2	42.35	-94.99	700.0	510.3	0.00	29	1982	2011
05482500	North Raccoon River near Jefferson (35)	2	41.99	-94.38	1,619.0	1,143.0	0.00	29	1982	2011
05483450	Middle Raccoon River near Bayard (36)	2	41.78	-94.49	375.0	269.3	0.00	29	1982	2011
05484000	South Raccoon River at Redfield (37)	3	41.59	-94.15	994.0	679.3	0.00	29	1982	2011
05484500	Raccoon River at Van Meter (38)	3	41.53	-93.95	3,441.0	2,406.5	0.00	29	1982	2011
05486000	North River near Norwalk (39)	1	41.46	-93.65	349.0	239.4	0.03	29	1982	2011
05486490	Middle River near Indianola (40)	3	41.42	-93.59	489.0	350.3	0.00	29	1982	2011
05487470	South River near Ackworth (41)	2	41.34	-93.49	460.0	306.2	0.00	29	1982	2011
05487980	White Breast Creek near Dallas (42)	1	41.25	-93.29	333.0	263.1	0.00	29	1982	2011
05488200	English Creek near Knoxville (43)	1	41.30	-93.05	90.1	71.8	0.33	26	1985	2011
05489000	Cedar Creek near Bussey (44)	2	41.22	-92.91	374.0	286.8	0.02	29	1982	2011

Appendix 2. Basin Characteristics Used in Analysis

Appendix 2. Description of all basin characteristics considered as potential explanatory variables in the development of the regressions conducted as part of the model comparison in the Des Moines and Iowa River Basins.

[USGS, U.S. Geological Survey; DEM, digital elevation model; WBD, watershed boundary dataset; m, meters; 24K, 1:24,000-scale; NHD, national hydrography dataset; GIS, geographic information system; NRSC, Natural Resource Conservation Service; SSURGO, Soil Survey Geographic database; IDNR, Iowa Department of Natural Resources; PRISM, parameter-elevation regressions on independent slopes model]

Morphometric characteristics	Source
DRNAREA—Drainage area (square miles)	USGS DEM (10 m), WBD (24k)
BASINPERIM—Basin perimeter (miles)	USGS DEM (10 m), WBD (24k)
BASLEN—Basin length (miles)	USGS DEM (150 m), WBD (24k)
BSLDEM10M—Average basin slope computed from 10 meter DEM (percent)	USGS DEM (10 m)
RELIEF—Basin relief computed as maximum elevation minus minimum elevation (feet)	USGS DEM (10 m)
RELRELF—Relative relief computed as RELIEF divided by BASINPERIM (feet per mile)	USGS DEM (10 m), WBD (24k)
BSHAPE—Shape factor measure of basin shape computed as BASLEN squared divided by DRNAREA (dimensionless)	USGS DEM (10 m), WBD (24k)
ELONRATIO—Elongation ratio measure of basin shape (dimensionless) (Eash, 2001)	USGS DEM (10 m), WBD (24k)
ROTUND—Rotundity of basin measure of basin shape (dimensionless) (Eash, 2001)	USGS DEM (10 m), WBD (24k)
COMPRAT—Compactness ratio measure of basin shape (dimensionless) (Eash, 2001)	USGS DEM (10 m), WBD (24k)
LENGTH—Main-channel length as measured from basin outlet to basin divide (miles)	USGS DEM NHD (24k)
MCSR—Main-channel sinuosity ratio computed as LENGTH divided by BASLEN (dimensionless)	USGS DEM (10 m), WBD, NHD (24k)
STRMTOT—Total length of mapped streams in basin (miles)	USGS DEM NHD (24k)
STRDEN—Stream density computed as STRMTOT divided by DRNAREA (miles per square mile)	USGS DEM (10 m), WBD, NHD (24k)
SLENRAT—Slenderness ratio computed as LENGTH squared divided by DRNAREA (dimensionless)	USGS DEM (10 m), WBD, NHD (24k)
CCM—Constant of channel maintenance computed as DRNAREA divided by STRMTOT (square miles per mile)	USGS DEM (10 m), WBD, NHD (24k)
CSL1085LFP—Stream slope computed as the change in elevation between points 10 and 85 percent of length along the longest flow path determined by a GIS divided by length between the points (feet per mile)	USGS DEM (10 m), NHD (24k)
CSL100—Stream slope computed as entire LENGTH (feet per mile)	USGS DEM (10 m), NHD (24k)
MCSP—Main-channel slope proportion computed as LENGTH divided by the square root of CSL1085LFP (dimensionless)	USGS DEM (10 m), NHD (24k)
RUGGED—Ruggedness number computed as STRMTOT multiplied by RELIEF and divided by DRNAREA (feet per mile)	USGS DEM (10 m), WBD, NHD (24k)
SLOPERAT—Slope ratio computed as CSL1085LFP divided by BSLDEM10M (dimensionless)	USGS DEM (10 m), NHD (24k)
FOSTREAM—Number of first-order streams within basin using the Strahler stream ordering method (dimensionless)	USGS DEM NHD (24k)
DRNFREQ—Drainage frequency computed as FOSTREAM divided by DRNAREA (number of first-order streams per square mile)	USGS DEM (10 m), WBD, NHD (24k)
RSD—Relative stream density computed as FOSTREAM multiplied by DRNAREA and divided by STRMTOT squared (dimensionless)	USGS DEM (10 m), WBD, NHD (24k)
SLOP30—Percent area with slopes greater than 30 percent	USGS DEM (10 m)
NFSL30—Percent area with slopes greater than 30 percent facing north	USGS DEM (10 m)
Hydrologic characteristics	Source
BFI—Base-flow index is the mean ratio of base flow to annual streamflow (dimensionless) (Wahl and Wahl, 1988)	USGS kriged BFI grid
HYSEP—Hydrograph separation and analysis is the median percentage of baseflow to annual streamflow (percent) (Sloto and Crouse, 1996)	USGS kriged HYSEP grid
TAU_ANN—Annual base-flow recession time constant computes the rate of baseflow recession between storms (days) (Eng and Milly, 2007)	USGS kriged TAU_ANN grid
STREAM_VAR—Streamflow-variability index is a measure of the steepness of the slope of a duration curve (dimensionless) (Koltun and Whitehead, 2002)	USGS kriged STREAM_VAR grid
Pedologic/geologic/land-use characteristics	Source
SOILASSURGO—Percent area underlain by hydrologic soil type A (percent area)	NRCS SSURGO Web Soil Survey
SOILBSSURGO—Percent area underlain by hydrologic soil type B (percent area)	NRCS SSURGO Web Soil Survey
SOILCSSURGO—Percent area underlain by hydrologic soil type C (percent area)	NRCS SSURGO Web Soil Survey
SOILDSSURGO—Percent area underlain by hydrologic soil type D (percent area)	NRCS SSURGO Web Soil Survey
SAND—Percent volume of sand content of soil (percent volume)	NRCS SSURGO Web Soil Survey
CLAY—Percent volume of clay content of soil (percent volume)	NRCS SSURGO Web Soil Survey
KSATSSUR—Average saturated hydraulic conductivity of soil (micrometers per second)	NRCS SSURGO Web Soil Survey
DESMOIN—Percent area of basin within Des Moines Lobe landform region (percent area)	Iowa Geological & Water Survey, IDNR grid
ROWCROP—Percent area of cultivated crops (percent area), see Web page: http://www.mrlc.gov/index.php , and Homer and others (2004)	2001 National Landcover Database grid

Appendix 2. Description of all basin characteristics considered as potential explanatory variables in the development of the regressions conducted as part of the model comparison in the Des Moines and Iowa River Basins.—Continued

[USGS, U.S. Geological Survey; DEM, digital elevation model; WBD, watershed boundary dataset; m, meters; 24K, 1:24,000-scale; NHD, national hydrography dataset; GIS, geographic information system; NRSC, Natural Resource Conservation Service; SSURGO, Soil Survey Geographic database; IDNR, Iowa Department of Natural Resources; PRISM, parameter-elevation regressions on independent slopes model]

Climatic characteristics	Source
PRECIP—Mean annual precipitation 1971–2000 (inches), see Web page: http://www.prism.oregonstate.edu/	PRISM Climate Group
I24H2Y—Maximum 24-hour precipitation that occurs on average once in 2 years	Midwest Climate Center Bulletin 71
I24H5Y—Maximum 24-hour precipitation that occurs on average once in 5 years	Midwest Climate Center Bulletin 71
I24H10Y—Maximum 24-hour precipitation that occurs on average once in 10 years	Midwest Climate Center Bulletin 71
I24H25Y—Maximum 24-hour precipitation that occurs on average once in 25 years	Midwest Climate Center Bulletin 71
I24H50Y—Maximum 24-hour precipitation that occurs on average once in 50 years	Midwest Climate Center Bulletin 71
I24h100Y—Maximum 24-hour precipitation that occurs on average once in 100 years	Midwest Climate Center Bulletin 71
PRC1—Mean January precipitation 1971–2000 (inches)	PRISM Climate Group
FEBAVPRE—Mean February precipitation 1971–2000 (inches)	PRISM Climate Group
MARAVPRE—Mean March precipitation 1971–2000 (inches)	PRISM Climate Group
PRC4—Mean April precipitation 1971–2000 (inches)	PRISM Climate Group
MAYAVEPRE—Mean May precipitation 1971–2000 (inches)	PRISM Climate Group
JUNEAVPRE—Mean June precipitation 1971–2000 (inches)	PRISM Climate Group
JULYAVPRE—Mean July precipitation 1971–2000 (inches)	PRISM Climate Group
PRC8—Mean August precipitation 1971–2000 (inches)	PRISM Climate Group
SEPAVPRE—Mean September precipitation 1971–2000 (inches)	PRISM Climate Group
OCTAVPRE—Mean October precipitation 1971–2000 (inches)	PRISM Climate Group
NOVAVPRE—Mean November precipitation 1971–2000 (inches)	PRISM Climate Group
DECAVPRE—Mean December precipitation 1971–2000 (inches)	PRISM Climate Group

Appendix 3. Cross-Validation of Map Correlation

Appendix 3. Leave-one-out cross-validated, root-mean-squared error of the fitted variograms of intersite hydrograph correlation at 44 streamgages in the Des Moines and Iowa River Basins.

Station number	Index number on figure 2	Root-mean- squared error
05449500	1	0.024
05451210	2	0.022
05451500	3	0.023
05451700	4	0.028
05451900	5	0.024
05452000	6	0.031
05452200	7	0.026
05453000	8	0.027
05453100	9	0.031
05454000	10	0.023
05454220	11	0.026
05454300	12	0.025
05455100	13	0.027
05455500	14	0.027
05457000	15	0.033
05457700	16	0.034
05458000	17	0.029
05458500	18	0.033
05458900	19	0.021
05459500	20	0.028
05462000	21	0.033
05463000	22	0.023
05463500	23	0.032
05464000	24	0.030
05464220	25	0.034
05464500	26	0.036
05465000	27	0.035
05476750	28	0.030
05479000	29	0.031
05480500	30	0.032
05481000	31	0.022
05481300	32	0.030
05481950	33	0.024
05482300	34	0.025
05482500	35	0.024
05483450	36	0.023
05484000	37	0.023
05484500	38	0.025
05486000	39	0.026
05486490	40	0.026
05487470	41	0.025
05487980	42	0.023
05488200	43	0.022
05489000	44	0.027

Appendix 4. Distributions of Each Performance Metric

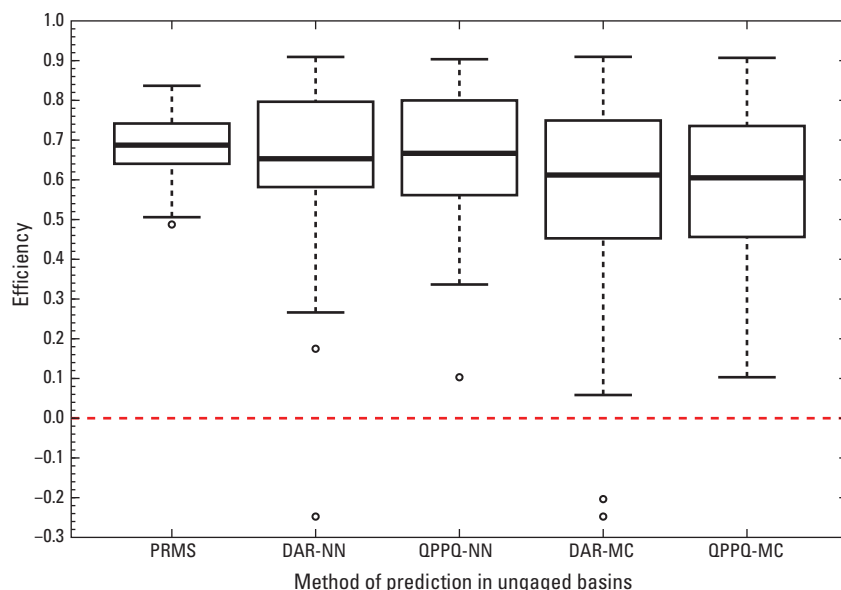


Figure 4-1. The distribution of the at-site Nash-Sutcliffe efficiencies of daily streamflow prediction for each method of prediction in ungauged basins (PUB) is considered here. The horizontal axis indicates each PUB method. The Nash-Sutcliffe efficiency is along the vertical axis. Nash-Sutcliffe efficiency ranges from one to negative infinity; a value of one indicates a perfect fit, while a value of zero indicates that a mean value would have produced the same level of accuracy. The dark line indicates the median of the distribution, the box outlines the 25th and 75th percentiles, and the whiskers extend to the data point a distance not more than 1.5 times the interquartile range away from the nearest quartile. The PUB methods include the Precipitation Runoff Modeling System (PRMS), drainage-area ratio with the nearest-neighboring index streamgauge (DAR-NN) or the map-correlated index streamgauge (DAR-MC), and nonlinear spatial interpolation using flow duration curves with the same index selection techniques (QPPQ-NN and QPPQ-MC).

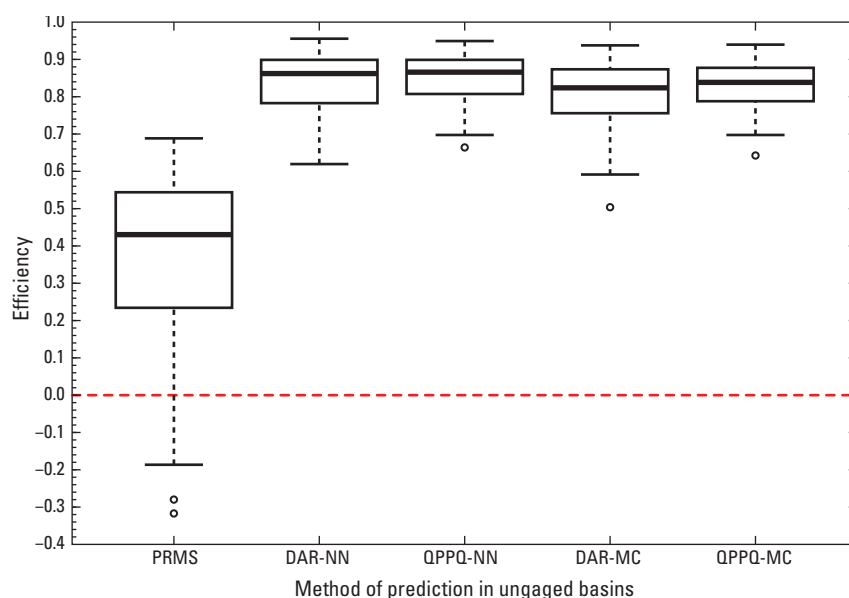


Figure 4-2. The distribution of the at-site Nash-Sutcliffe efficiencies of the logarithms of daily streamflow predictions for each method of prediction in ungauged basins (PUB) is considered here. The horizontal axis indicates each PUB method. The Nash-Sutcliffe efficiency of the logarithms is along the vertical axis. Nash-Sutcliffe efficiency ranges from one to negative infinity; a value of one indicates a perfect fit, while a value of zero indicates that a mean value would have produced the same level of accuracy. The dark line indicates the median of the distribution, the box outlines the 25th and 75th percentiles, and the whiskers extend to the data point a distance not more than 1.5 times the interquartile range away from the nearest quartile. The PUB methods include the Precipitation Runoff Modeling System (PRMS), drainage-area ratio with the nearest-neighboring index streamgauge (DAR-NN) or the map-correlated index streamgauge (DAR-MC), and nonlinear spatial interpolation using flow duration curves with the same index selection techniques (QPPQ-NN and QPPQ-MC).

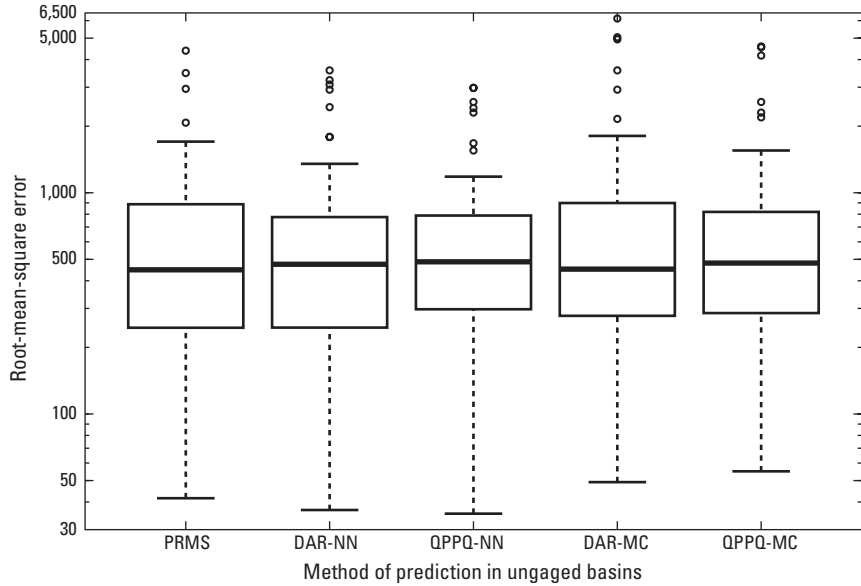


Figure 4-3. The distribution of the at-site root-mean-square errors of daily streamflow predictions for each method of prediction in ungauged basins (PUB) is considered here. The horizontal axis indicates each PUB method. The vertical axis indicates the root-mean-square error in units of streamflow. Lower values represent less error, on average. The dark line indicates the median of the distribution, the box outlines the 25th and 75th percentiles, and the whiskers extend to the data point a distance not more than 1.5 times the interquartile range away from the nearest quartile. The PUB methods include the Precipitation Runoff Modeling System (PRMS), drainage-area ratio with the nearest-neighboring index streamgauge (DAR-NN) or the map-correlated index streamgauge (DAR-MC), and nonlinear spatial interpolation using flow duration curves with the same index selection techniques (QPPQ-NN and QPPQ-MC).

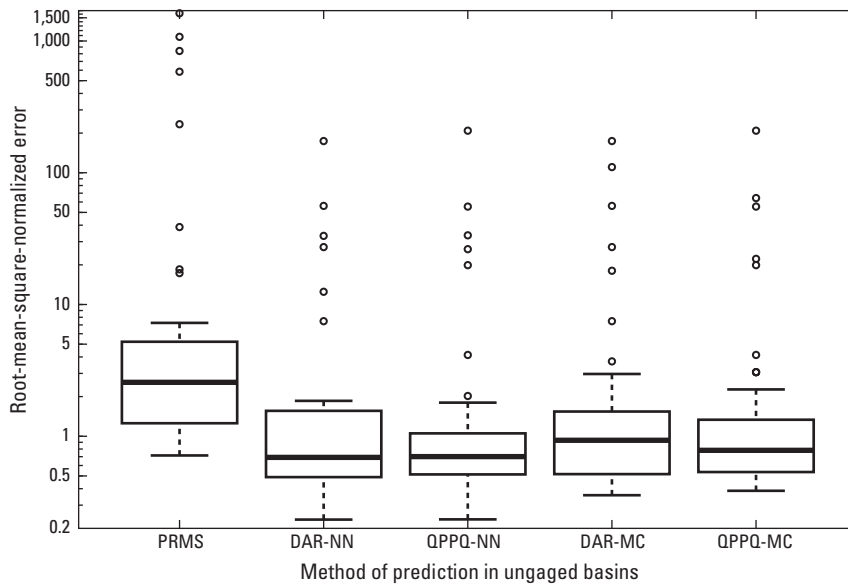


Figure 4-4. The distribution of the at-site root-mean-square-normalized errors of daily streamflow predictions for each method of prediction in ungauged basins (PUB) is considered here. The horizontal axis indicates each PUB method. The vertical axis indicates the root-mean-square-normalized error. Lower values represent less error, on average. The dark line indicates the median of the distribution, the box outlines the 25th and 75th percentiles, and the whiskers extend to the data point a distance not more than 1.5 times the interquartile range away from the nearest quartile. The PUB methods include the Precipitation Runoff Modeling System (PRMS), drainage-area ratio with the nearest-neighboring index streamgauge (DAR-NN) or the map-correlated index streamgauge (DAR-MC), and nonlinear spatial interpolation using flow duration curves with the same index selection techniques (QPPQ-NN and QPPQ-MC).

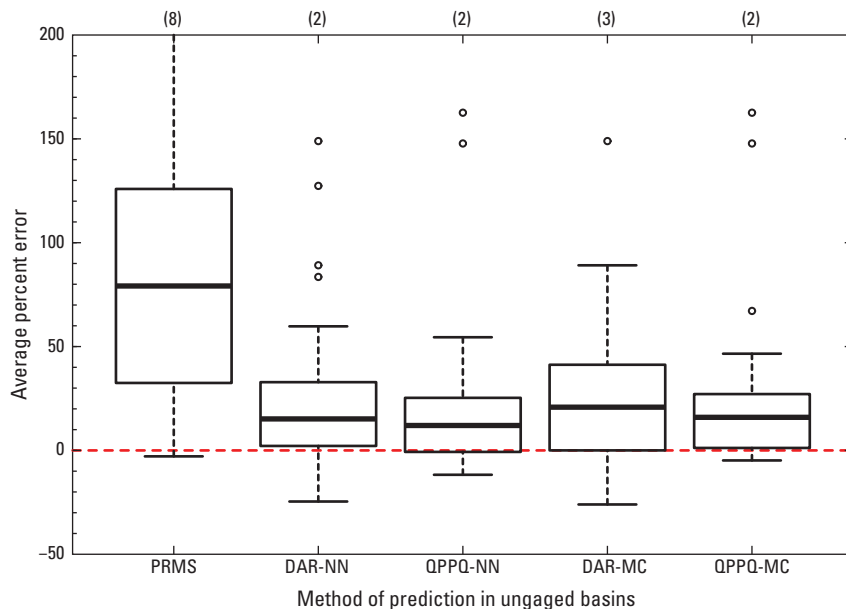


Figure 4-5. The distribution of at-site average percent errors of daily streamflow predictions for each method of prediction in ungaged basins (PUB) is considered here. The horizontal axis indicates each PUB method. The vertical axis shows the average percent bias. Unbiased methods display a median near zero and minimum variability of at-site bias. The dark line indicates the median of the distribution, the box outlines the 25th and 75th percentiles, and the whiskers extend to the data point a distance not more than 1.5 times the interquartile range away from the nearest quartile. Numbers at the top of the graph indicate outliers beyond the upper limit of the vertical axis. The PUB methods include the Precipitation Runoff Modeling System (PRMS), drainage-area ratio with the nearest-neighboring index streamgauge (DAR-NN) or the map-correlated index streamgauge (DAR-MC), and nonlinear spatial interpolation using flow duration curves with the same index selection techniques (QPPQ-NN and QPPQ-MC).

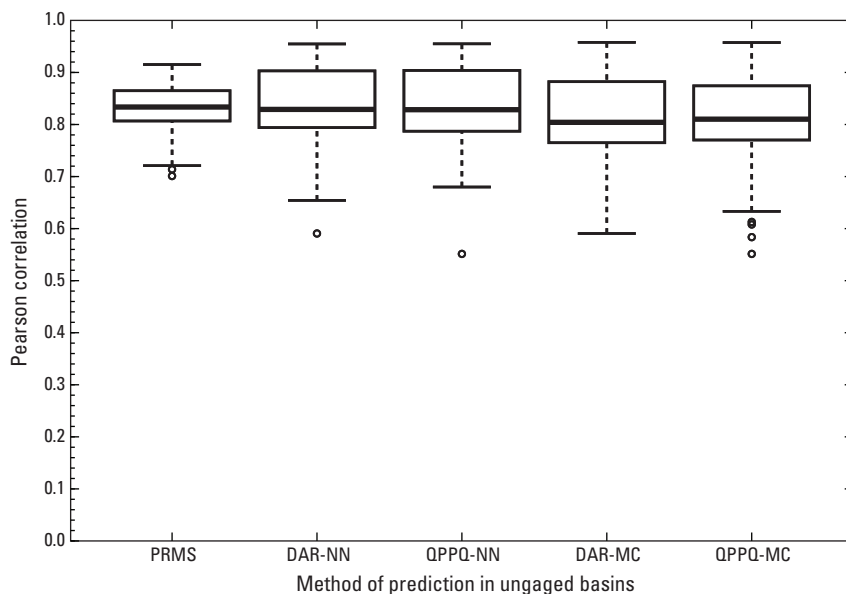


Figure 4-6. The distribution of at-site Pearson correlations between simulated and observed daily streamflows for each method of prediction in ungaged basins (PUB) is considered here. The horizontal axis indicates each PUB method. The vertical axis shows the Pearson correlation, which ranges from negative to positive one. A perfect correspondence would exhibit a Pearson correlation of one. The dark line indicates the median of the distribution, the box outlines the 25th and 75th percentiles, and the whiskers extend to the data point a distance not more than 1.5 times the interquartile range away from the nearest quartile. The PUB methods include the Precipitation Runoff Modeling System (PRMS), drainage-area ratio with the nearest-neighboring index streamgauge (DAR-NN) or the map-correlated index streamgauge (DAR-MC), and nonlinear spatial interpolation using flow duration curves with the same index selection techniques (QPPQ-NN and QPPQ-MC).

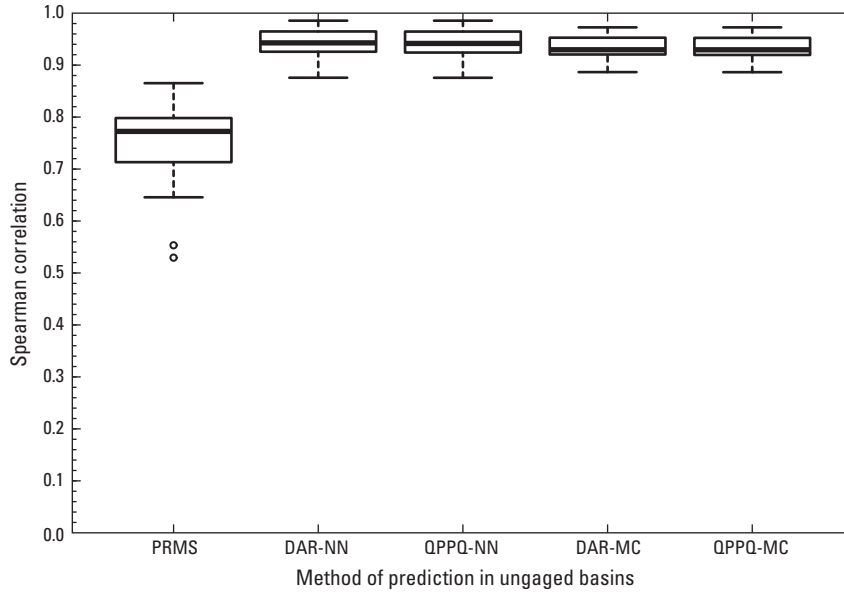


Figure 4-7. The distribution of at-site Spearman correlations between simulated and observed daily streamflows for each method of prediction in ungauged basins (PUB) is considered here. The horizontal axis indicates each PUB method. The vertical axis shows the Spearman correlation, which ranges from negative to positive one. A perfect correspondence between ranked streamflow would exhibit a Spearman correlation of one. The dark line indicates the median of the distribution, the box outlines the 25th and 75th percentiles, and the whiskers extend to the data point a distance not more than 1.5 times the interquartile range away from the nearest quartile. The PUB methods include the Precipitation Runoff Modeling System (PRMS), drainage-area ratio with the nearest-neighboring index streamgauge (DAR-NN) or the map-correlated index streamgauge (DAR-MC), and nonlinear spatial interpolation using flow duration curves with the same index selection techniques (QPPQ-NN and QPPQ-MC).

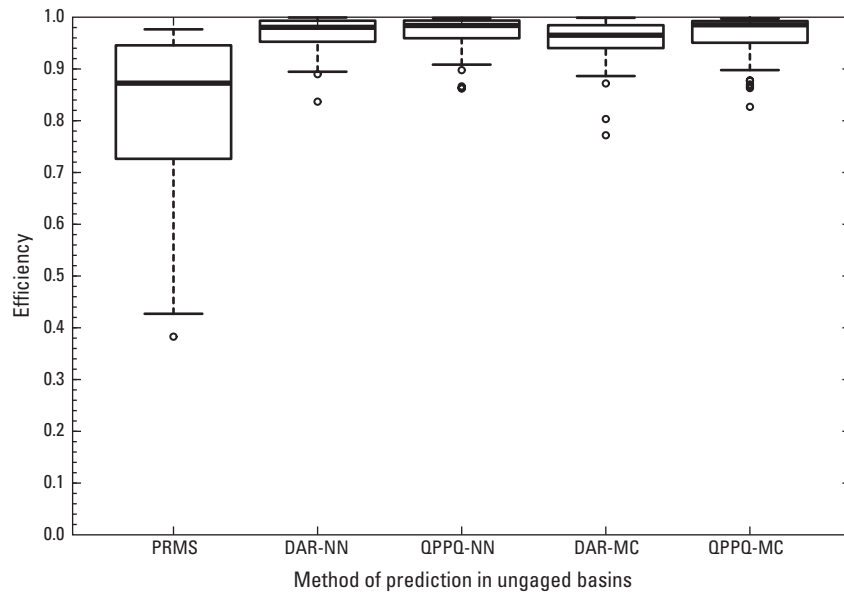


Figure 4-8. The distribution of the at-site Nash-Sutcliffe efficiencies of the daily storage-yield curve (SYC) for each method of prediction in ungauged basins (PUB) is considered here. See text for a description of the methodology used to predict the SYC. The horizontal axis indicates each PUB method. The Nash-Sutcliffe efficiency is along the vertical axis. Nash-Sutcliffe efficiency ranges from one to negative infinity; a value of one indicates a perfect fit, while a value of zero indicates that a mean value would have produced the same level of accuracy. The dark line indicates the median of the distribution, the box outlines the 25th and 75th percentiles, and the whiskers extend to the data point a distance not more than 1.5 times the interquartile range away from the nearest quartile. The PUB methods include the Precipitation Runoff Modeling System (PRMS), drainage-area ratio with the nearest-neighboring index streamgauge (DAR-NN) or the map-correlated index streamgauge (DAR-MC), and nonlinear spatial interpolation using flow duration curves with the same index selection techniques (QPPQ-NN and QPPQ-MC).

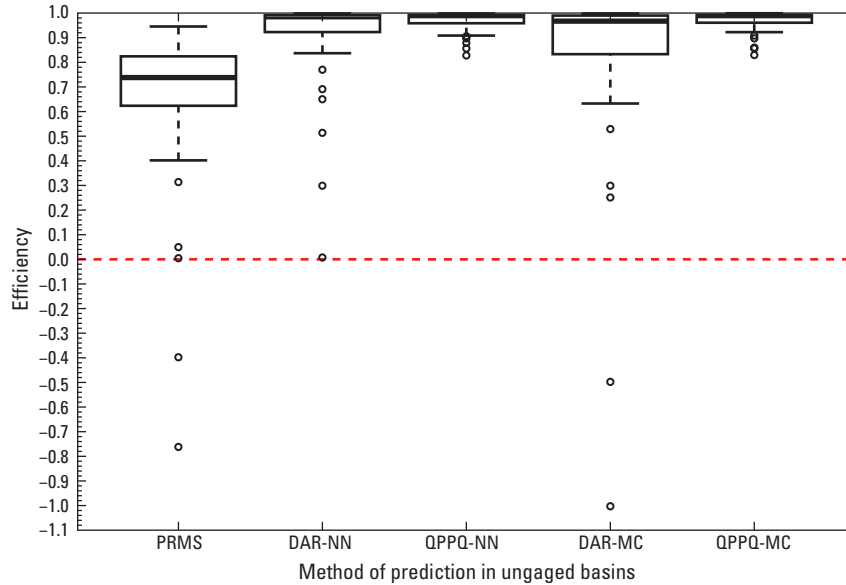


Figure 4-9. The distribution of the at-site Nash-Sutcliffe efficiencies of the logarithms of the daily storage-yield curve (SYC) for each method of prediction in ungaged basins (PUB) is considered here. See text for a description of the methodology used to predict the SYC. The horizontal axis indicates each PUB method. The Nash-Sutcliffe efficiency of the logarithms is along the vertical axis. Nash-Sutcliffe efficiency ranges from one to negative infinity; a value of one indicates a perfect fit, while a value of zero indicates that a mean value would have produced the same level of accuracy. The dark line indicates the median of the distribution, the box outlines the 25th and 75th percentiles, and the whiskers extend to the data point a distance not more than 1.5 times the interquartile range away from the nearest quartile. The PUB methods include the Precipitation Runoff Modeling System (PRMS), drainage-area ratio with the nearest-neighboring index streamgage (DAR-NN) or the map-correlated index streamgage (DAR-MC), and nonlinear spatial interpolation using flow duration curves with the same index selection techniques (QPPQ-NN and QPPQ-MC).

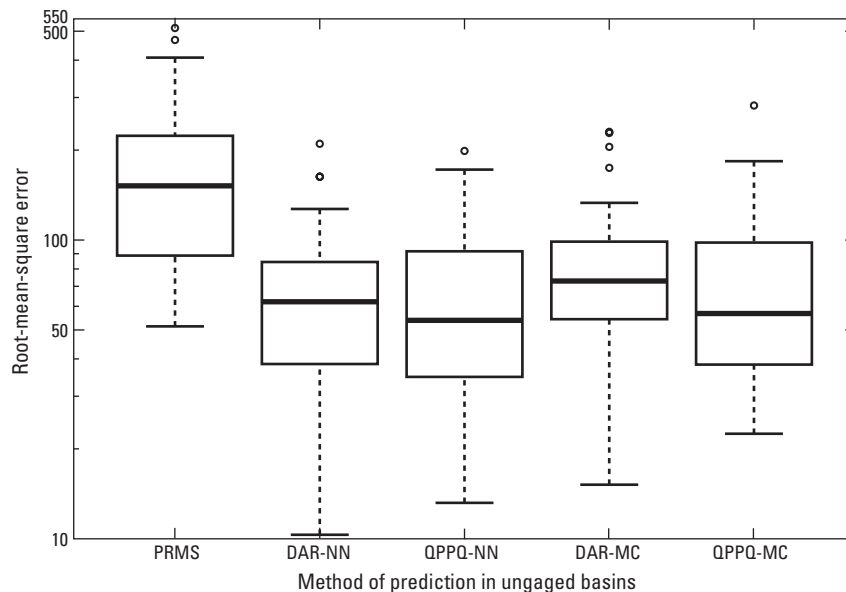


Figure 4-10. The distribution of the at-site root-mean-square errors of the daily storage-yield curve for each method of prediction in ungaged basins (PUB) is considered here. The horizontal axis indicates each PUB method. The vertical axis indicates the root-mean-square error in units of storage fraction (time, storage volume divided by mean streamflow). Lower values represent less error, on average. The dark line indicates the median of the distribution, the box outlines the 25th and 75th percentiles, and the whiskers extend to the data point a distance not more than 1.5 times the interquartile range away from the nearest quartile. The PUB methods include the Precipitation Runoff Modeling System (PRMS), drainage-area ratio with the nearest-neighboring index streamgage (DAR-NN) or the map-correlated index streamgage (DAR-MC), and nonlinear spatial interpolation using flow duration curves with the same index selection techniques (QPPQ-NN and QPPQ-MC).

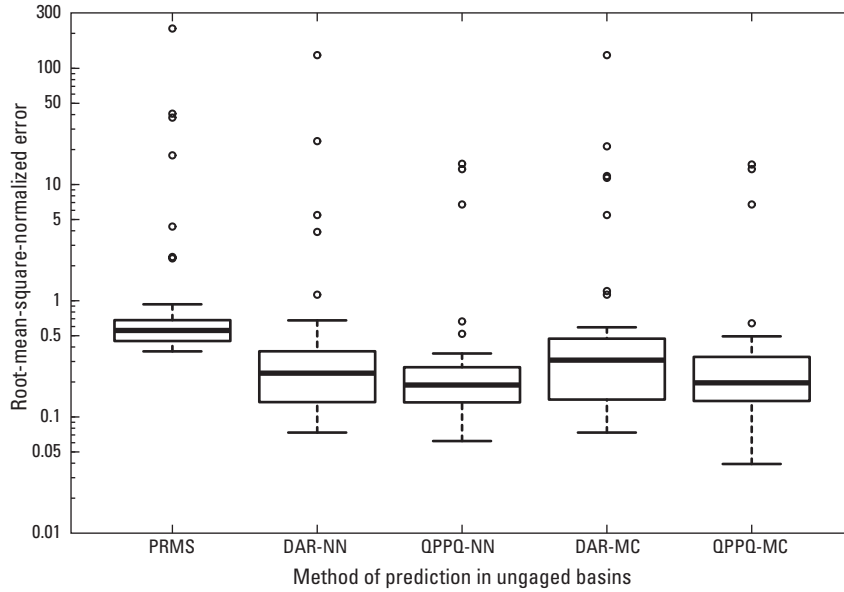


Figure 4–11. The distribution of the at-site root-mean-square-normalized errors of the daily storage-yield curve for each method of prediction in ungauged basins (PUB) is considered here. The horizontal axis indicates each PUB method. The vertical axis indicates the root-mean-square-normalized error. Lower values represent less error, on average. The dark line indicates the median of the distribution, the box outlines the 25th and 75th percentiles, and the whiskers extend to the data point a distance not more than 1.5 times the interquartile range away from the nearest quartile. The PUB methods include the Precipitation Runoff Modeling System (PRMS), drainage-area ratio with the nearest-neighboring index streamgauge (DAR-NN) or the map-correlated index streamgauge (DAR-MC), and nonlinear spatial interpolation using flow duration curves with the same index selection techniques (QPPQ-NN and QPPQ-MC).

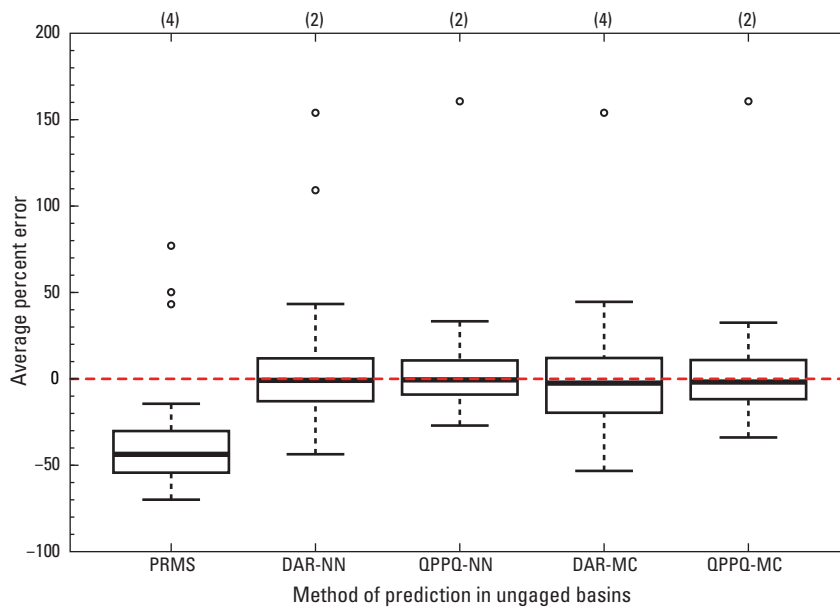


Figure 4–12. The distribution of at-site average percent errors of the daily storage-yield curve for each method of prediction in ungauged basins (PUB) is considered here. The horizontal axis indicates each PUB method. The vertical axis shows the average percent bias. Unbiased methods display a median near zero and minimum variability of at-site bias. The dark line indicates the median of the distribution, the box outlines the 25th and 75th percentiles, and the whiskers extend to the data point a distance not more than 1.5 times the interquartile range away from the nearest quartile. Numbers at the top of the graph indicate outliers beyond the upper limit of the vertical axis. The PUB methods include the Precipitation Runoff Modeling System (PRMS), drainage-area ratio with the nearest-neighboring index streamgauge (DAR-NN) or the map-correlated index streamgauge (DAR-MC), and nonlinear spatial interpolation using flow duration curves with the same index selection techniques (QPPQ-NN and QPPQ-MC).

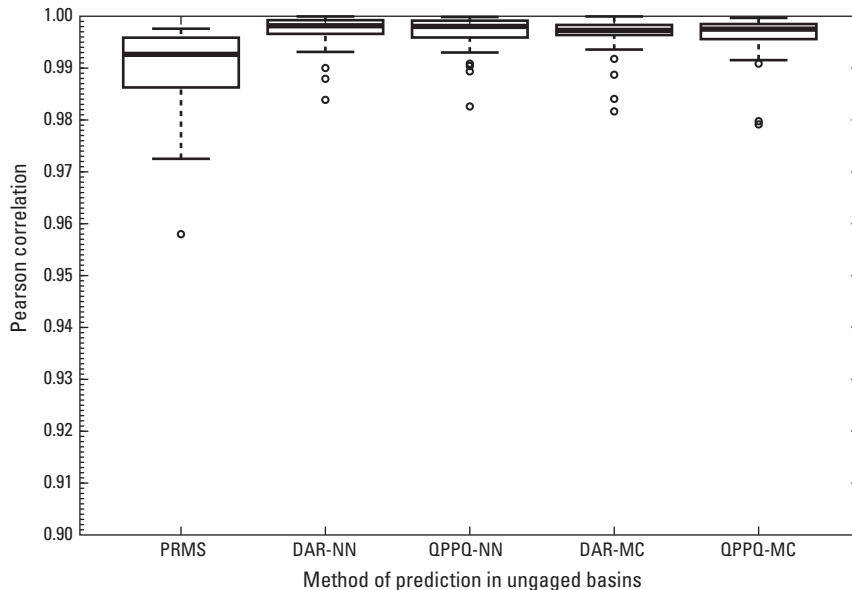


Figure 4–13. The distribution of at-site Pearson correlations between the simulated and observed daily storage-yield curves for each method of prediction in ungaged basins (PUB) is considered here. The horizontal axis indicates each PUB method. The vertical axis shows the Pearson correlation, which ranges from negative to positive one. A perfect correspondence would exhibit a Pearson correlation of one. The dark line indicates the median of the distribution, the box outlines the 25th and 75th percentiles, and the whiskers extend to the data point a distance not more than 1.5 times the interquartile range away from the nearest quartile. The PUB methods include the Precipitation Runoff Modeling System (PRMS), drainage-area ratio with the nearest-neighboring index streamgauge (DAR-NN) or the map-correlated index streamgauge (DAR-MC), and nonlinear spatial interpolation using flow duration curves with the same index selection techniques (QPPQ-NN and QPPQ-MC).

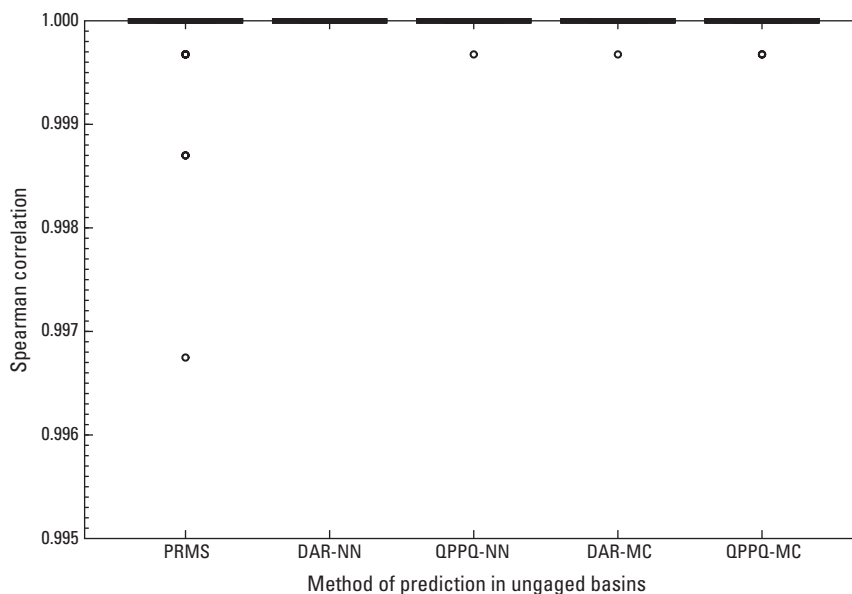


Figure 4–14. The distribution of at-site Spearman correlations between the simulated and observed daily storage-yield curves for each method of prediction in ungaged basins (PUB) is considered here. The horizontal axis indicates each PUB method. The vertical axis shows the Spearman correlation, which ranges from negative to positive one. A perfect correspondence between ranked values would exhibit a Spearman correlation of one. The dark line indicates the median of the distribution, the box outlines the 25th and 75th percentiles, and the whiskers extend to the data point a distance not more than 1.5 times the interquartile range away from the nearest quartile. The PUB methods include the Precipitation Runoff Modeling System (PRMS), drainage-area ratio with the nearest-neighboring index streamgauge (DAR-NN) or the map-correlated index streamgauge (DAR-MC), and nonlinear spatial interpolation using flow duration curves with the same index selection techniques (QPPQ-NN and QPPQ-MC). NOTE: The boxes are compressed because most values are one.

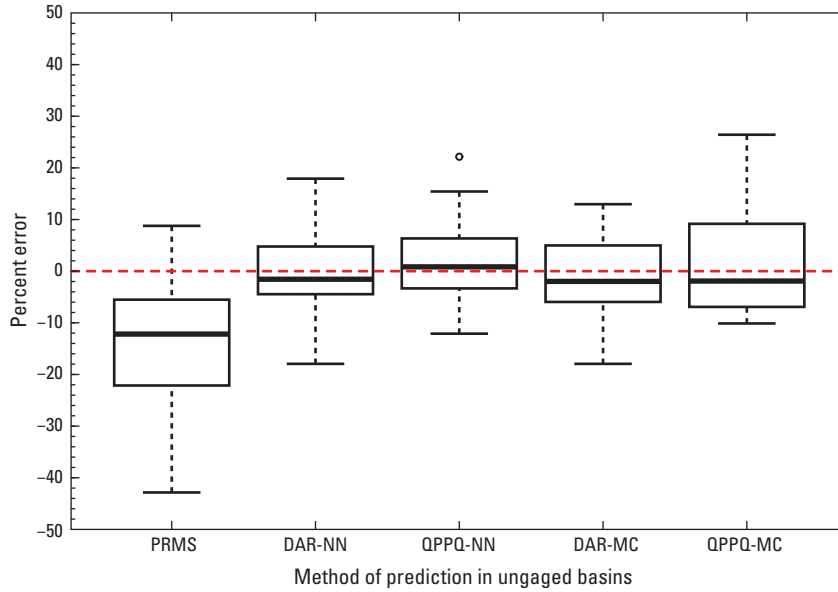


Figure 4-15. The distribution of at-site percent errors in the estimated coefficient of variation of annual streamflows for each method of prediction in ungaged basins (PUB) is considered here. The horizontal axis indicates each PUB method. The vertical axis shows the percent error. Unbiased methods display a median near zero and minimum variability of at-site bias. The dark line indicates the median of the distribution, the box outlines the 25th and 75th percentiles, and the whiskers extend to the data point a distance not more than 1.5 times the interquartile range away from the nearest quartile. The PUB methods include the Precipitation Runoff Modeling System (PRMS), drainage-area ratio with the nearest-neighboring index streamgauge (DAR-NN) or the map-correlated index streamgauge (DAR-MC), and nonlinear spatial interpolation using flow duration curves with the same index selection techniques (QPPQ-NN and QPPQ-MC).

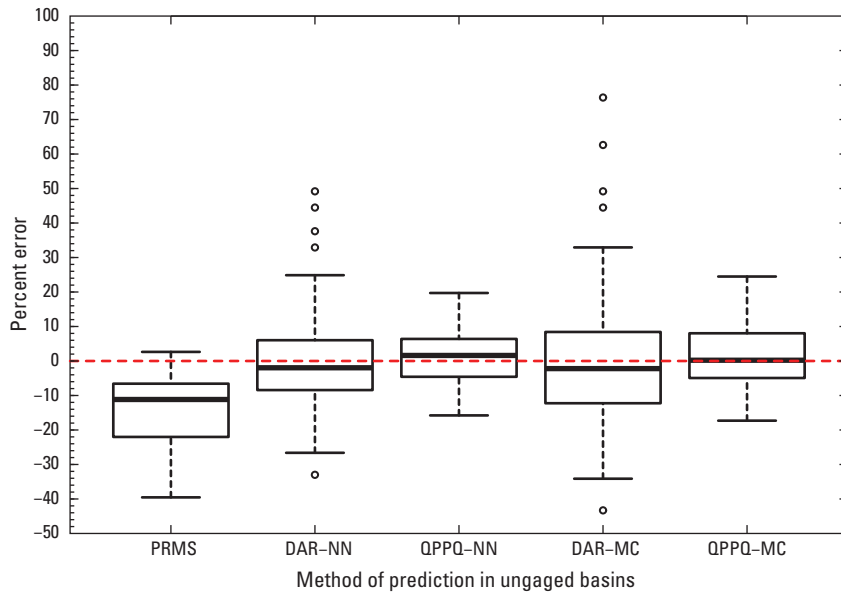


Figure 4-16. The distribution of at-site percent errors in the estimated coefficient of variation of daily streamflows for each method of prediction in ungaged basins (PUB) is considered here. The horizontal axis indicates each PUB method. The vertical axis shows the percent error. Unbiased methods display a median near zero and minimum variability of at-site bias. The dark line indicates the median of the distribution, the box outlines the 25th and 75th percentiles, and the whiskers extend to the data point a distance not more than 1.5 times the interquartile range away from the nearest quartile. The PUB methods include the Precipitation Runoff Modeling System (PRMS), drainage-area ratio with the nearest-neighboring index streamgauge (DAR-NN) or the map-correlated index streamgauge (DAR-MC), and nonlinear spatial interpolation using flow duration curves with the same index selection techniques (QPPQ-NN and QPPQ-MC).

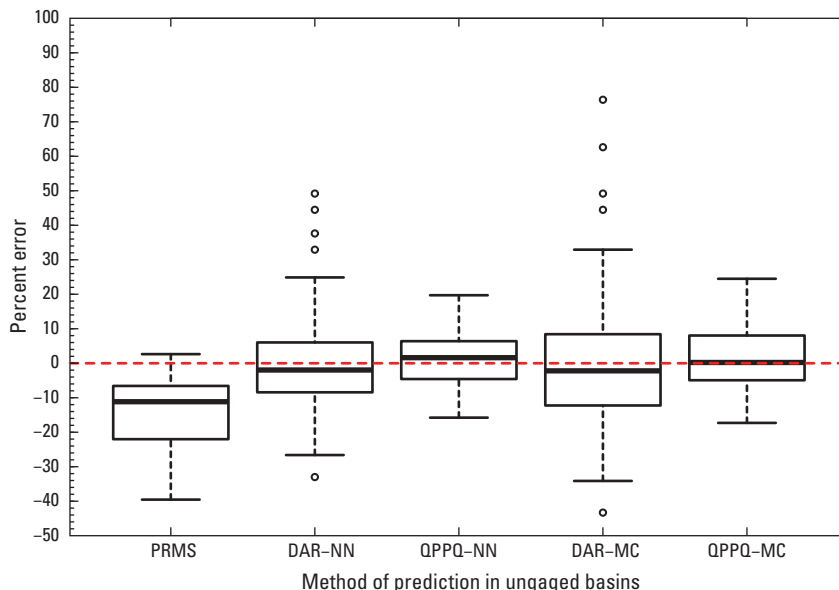


Figure 4–17. The distribution of at-site percent errors in the estimated 10th percentile of the distribution of 7-day average annual-minimum events for each method of prediction in ungaged basins (PUB) is considered here. This event is related to the 10-year, 7-day average annual event. The horizontal axis indicates each PUB method. The vertical axis shows the percent error. Unbiased methods display a median near zero and minimum variability of at-site bias. The dark line indicates the median of the distribution, the box outlines the 25th and 75th percentiles, and the whiskers extend to the data point a distance not more than 1.5 times the interquartile range away from the nearest quartile. Numbers at the top of the graph indicate outliers beyond the upper limit of the vertical axis. The PUB methods include the Precipitation Runoff Modeling System (PRMS), drainage-area ratio with the nearest-neighboring index streamgauge (DAR-NN) or the map-correlated index streamgauge (DAR-MC), and nonlinear spatial interpolation using flow duration curves with the same index selection techniques (QPPQ-NN and QPPQ-MC).

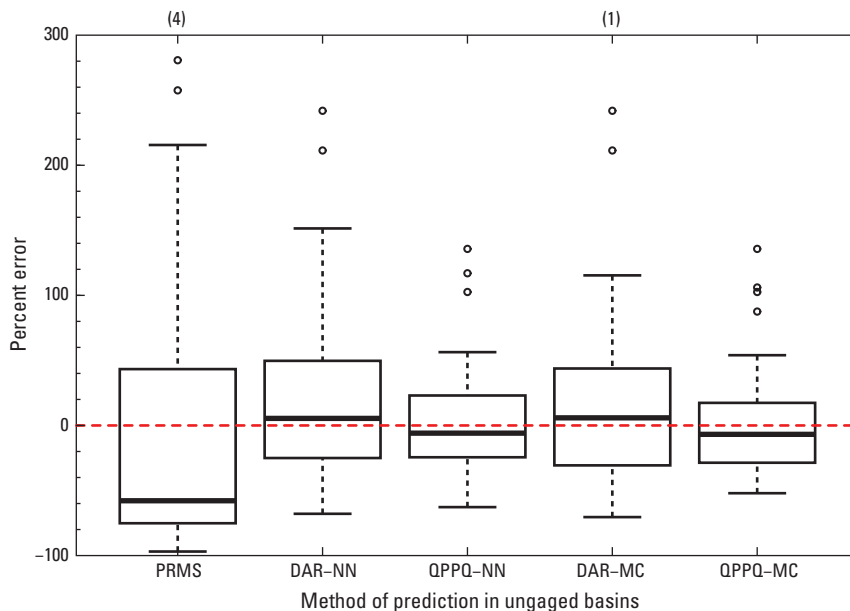


Figure 4–18. The distribution of at-site percent errors in the estimated 50th percentile of the distribution of 7-day average annual-minimum events for each method of prediction in ungaged basins (PUB) is considered here. This event is related to the 2-year, 7-day annual-minimum event. The horizontal axis indicates each PUB method. The vertical axis shows the percent error. Unbiased methods display a median near zero and minimum variability of at-site bias. The dark line indicates the median of the distribution, the box outlines the 25th and 75th percentiles, and the whiskers extend to the data point a distance not more than 1.5 times the interquartile range away from the nearest quartile. Numbers at the top of the graph indicate outliers beyond the upper limit of the vertical axis. The PUB methods include the Precipitation Runoff Modeling System (PRMS), drainage-area ratio with the nearest-neighboring index streamgauge (DAR-NN) or the map-correlated index streamgauge (DAR-MC), and nonlinear spatial interpolation using flow duration curves with the same index selection techniques (QPPQ-NN and QPPQ-MC).

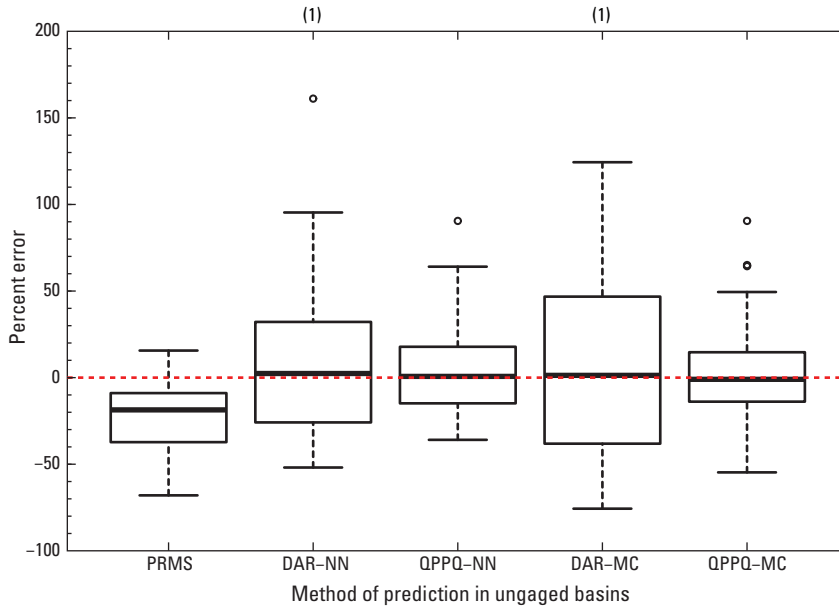


Figure 4–19. The distribution of at-site percent errors in the estimated 90th percentile of the distribution of annual-maximum events for each method of prediction in ungaged basins (PUB) is considered here. This event is related to the 10-year annual-maximum event. The horizontal axis indicates each PUB method. The vertical axis shows the percent error. Unbiased methods display a median near zero and minimum variability of at-site bias. The dark line indicates the median of the distribution, the box outlines the 25th and 75th percentiles, and the whiskers extend to the data point a distance not more than 1.5 times the interquartile range away from the nearest quartile. Numbers at the top of the graph indicate outliers beyond the upper limit of the vertical axis. The PUB methods include the Precipitation Runoff Modeling System (PRMS), drainage-area ratio with the nearest-neighboring index streamgage (DAR-NN) or the map-correlated index streamgage (DAR-MC), and nonlinear spatial interpolation using flow duration curves with the same index selection techniques (QPPQ-NN and QPPQ-MC).

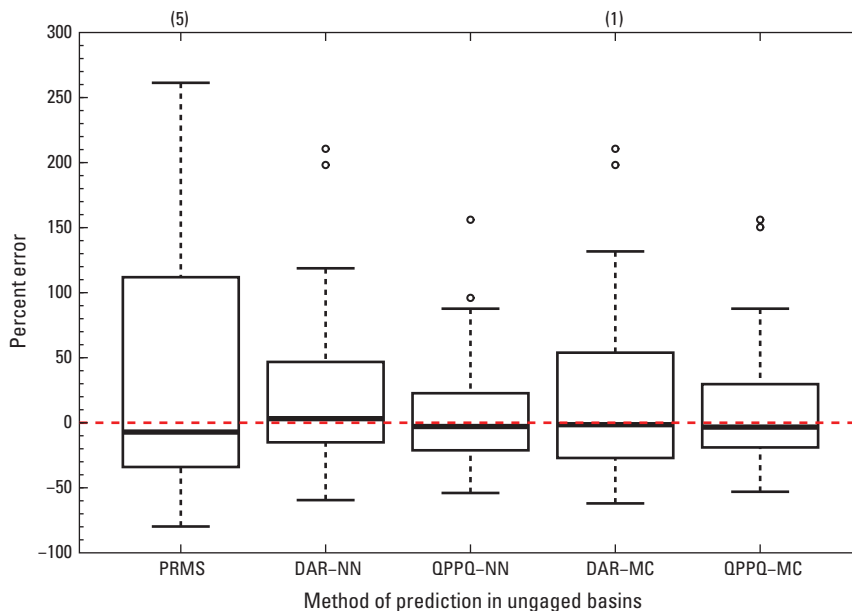


Figure 4–20. The distribution of at-site percent errors in the estimated 90-percent-exceedance streamflow for each method of prediction in ungaged basins (PUB) is considered here. The horizontal axis indicates each PUB method. The vertical axis shows the percent error. Unbiased methods display a median near zero and minimum variability of at-site bias. The dark line indicates the median of the distribution, the box outlines the 25th and 75th percentiles, and the whiskers extend to the data point a distance not more than 1.5 times the interquartile range away from the nearest quartile. Numbers at the top of the graph indicate outliers beyond the upper limit of the vertical axis. The PUB methods include the Precipitation Runoff Modeling System (PRMS), drainage-area ratio with the nearest-neighboring index streamgage (DAR-NN) or the map-correlated index streamgage (DAR-MC), and nonlinear spatial interpolation using flow duration curves with the same index selection techniques (QPPQ-NN and QPPQ-MC).

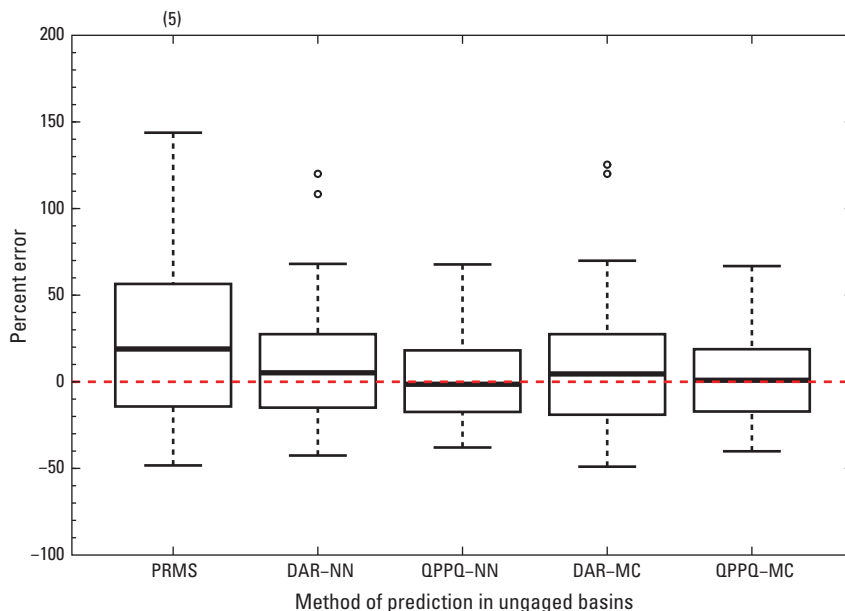


Figure 4-21. The distribution of at-site percent errors in the estimated 75-percent-exceedance streamflow for each method of prediction in ungaged basins (PUB) is considered here. The horizontal axis indicates each PUB method. The vertical axis shows the percent error. Unbiased methods display a median near zero and minimum variability of at-site bias. The dark line indicates the median of the distribution, the box outlines the 25th and 75th percentiles, and the whiskers extend to the data point a distance not more than 1.5 times the interquartile range away from the nearest quartile. Numbers at the top of the graph indicate outliers beyond the upper limit of the vertical axis. The PUB methods include the Precipitation Runoff Modeling System (PRMS), drainage-area ratio with the nearest-neighboring index streamgauge (DAR-NN) or the map-correlated index streamgauge (DAR-MC), and nonlinear spatial interpolation using flow duration curves with the same index selection techniques (QPPQ-NN and QPPQ-MC).

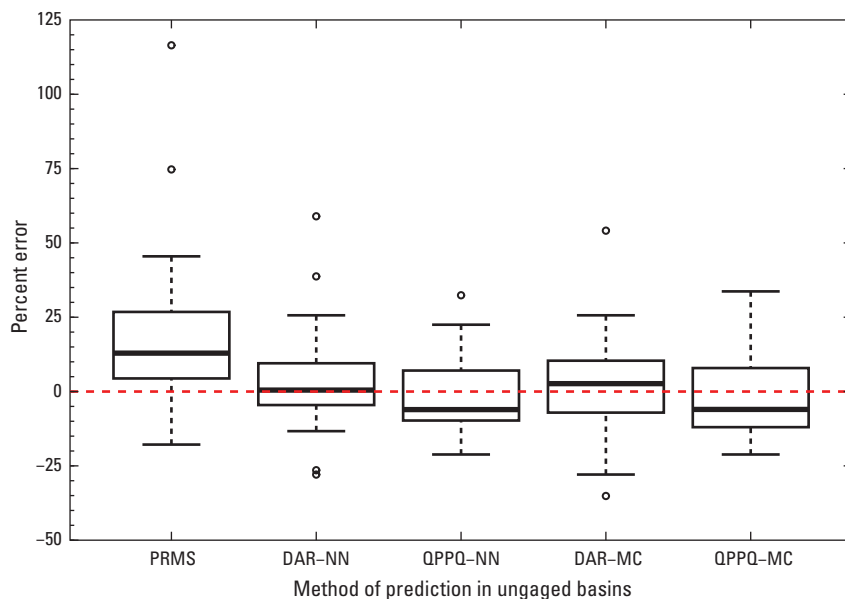


Figure 4-22. The distribution of at-site percent errors in the estimated 50-percent-exceedance streamflow for each method of prediction in ungaged basins (PUB) is considered here. The horizontal axis indicates each PUB method. The vertical axis shows the percent error. Unbiased methods display a median near zero and minimum variability of at-site bias. The dark line indicates the median of the distribution, the box outlines the 25th and 75th percentiles, and the whiskers extend to the data point a distance not more than 1.5 times the interquartile range away from the nearest quartile. The PUB methods include the Precipitation Runoff Modeling System (PRMS), drainage-area ratio with the nearest-neighboring index streamgauge (DAR-NN) or the map-correlated index streamgauge (DAR-MC), and nonlinear spatial interpolation using flow duration curves with the same index selection techniques (QPPQ-NN and QPPQ-MC).

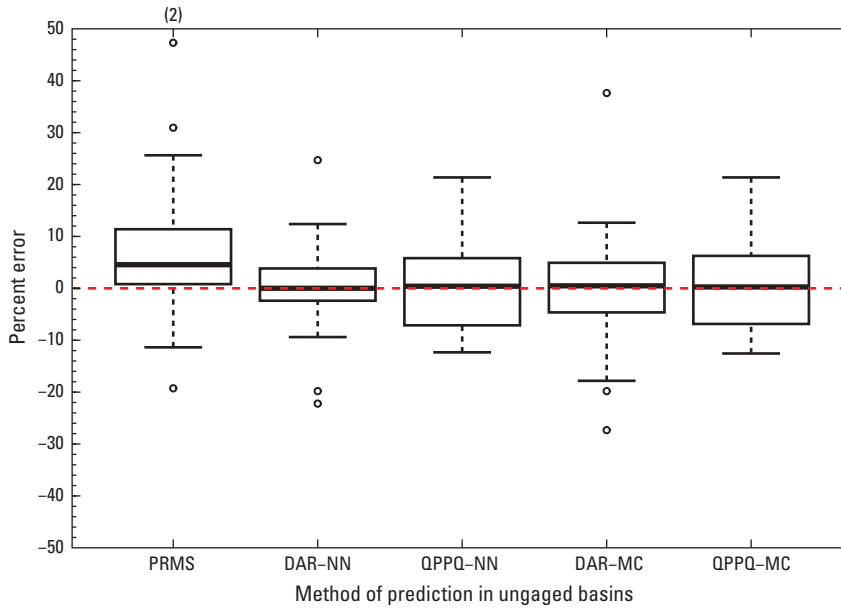


Figure 4-23. The distribution of at-site percent errors in the estimated 25-percent-exceedance streamflow for each method of prediction in ungaged basins (PUB) is considered here. The horizontal axis indicates each PUB method. The vertical axis shows the percent error. Unbiased methods display a median near zero and minimum variability of at-site bias. The dark line indicates the median of the distribution, the box outlines the 25th and 75th percentiles, and the whiskers extend to the data point a distance not more than 1.5 times the interquartile range away from the nearest quartile. Numbers at the top of the graph indicate outliers beyond the upper limit of the vertical axis. The PUB methods include the Precipitation Runoff Modeling System (PRMS), drainage-area ratio with the nearest-neighboring index streamgauge (DAR-NN) or the map-correlated index streamgauge (DAR-MC), and nonlinear spatial interpolation using flow duration curves with the same index selection techniques (QPPQ-NN and QPPQ-MC).

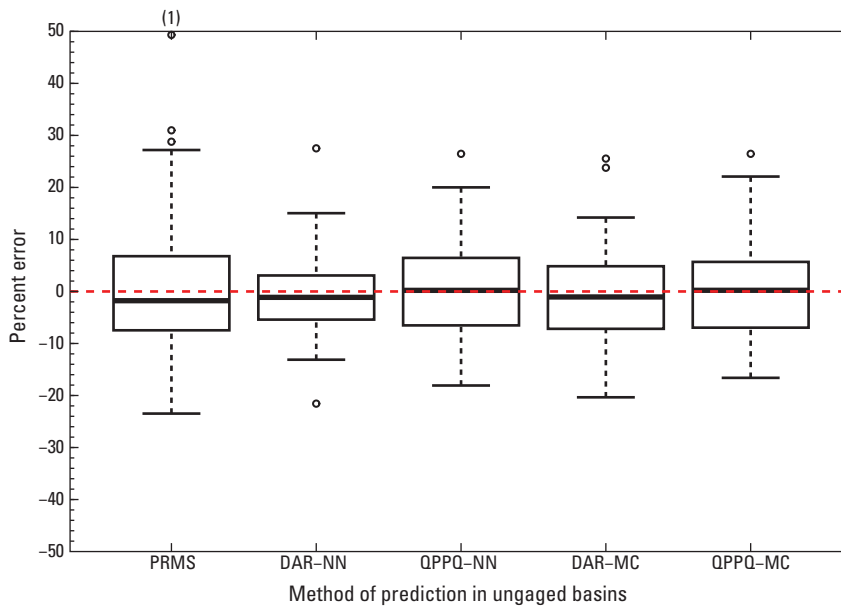


Figure 4-24. The distribution of at-site percent errors in the estimated 10-percent-exceedance streamflow for each method of prediction in ungaged basins (PUB) is considered here. The horizontal axis indicates each PUB method. The vertical axis shows the percent error. Unbiased methods display a median near zero and minimum variability of at-site bias. The dark line indicates the median of the distribution, the box outlines the 25th and 75th percentiles, and the whiskers extend to the data point a distance not more than 1.5 times the interquartile range away from the nearest quartile. Numbers at the top of the graph indicate outliers beyond the upper limit of the vertical axis. The PUB methods include the Precipitation Runoff Modeling System (PRMS), drainage-area ratio with the nearest-neighboring index streamgauge (DAR-NN) or the map-correlated index streamgauge (DAR-MC), and nonlinear spatial interpolation using flow duration curves with the same index selection techniques (QPPQ-NN and QPPQ-MC).

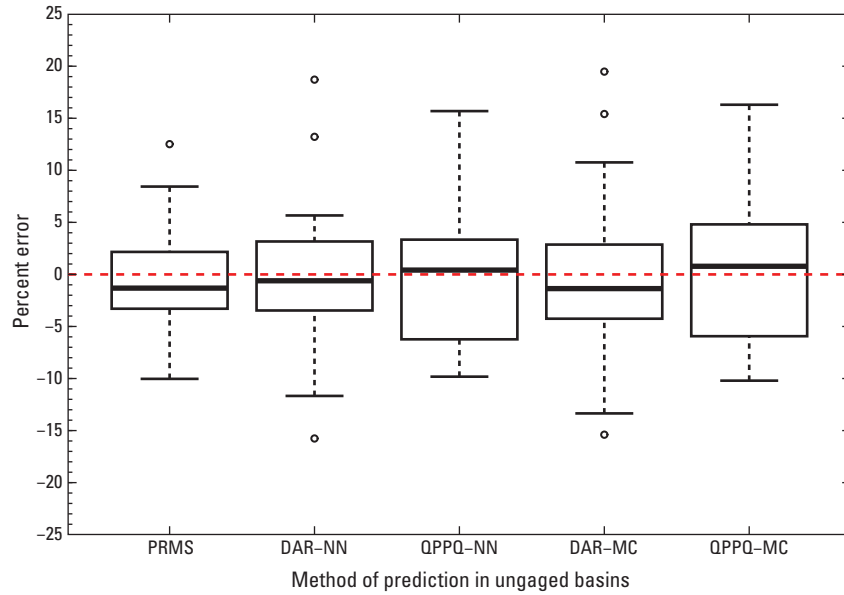


Figure 4–25. The distribution of at-site percent errors in the estimated mean daily streamflow for each method of prediction in ungaged basins (PUB) is considered here. The horizontal axis indicates each PUB method. The vertical axis shows the percent error. Unbiased methods display a median near zero and minimum variability of at-site bias. The dark line indicates the median of the distribution, the box outlines the 25th and 75th percentiles, and the whiskers extend to the data point a distance not more than 1.5 times the interquartile range away from the nearest quartile. The PUB methods include the Precipitation Runoff Modeling System (PRMS), drainage-area ratio with the nearest-neighboring index streamgauge (DAR-NN) or the map-correlated index streamgauge (DAR-MC), and nonlinear spatial interpolation using flow duration curves with the same index selection techniques (QPPQ-NN and QPPQ-MC).

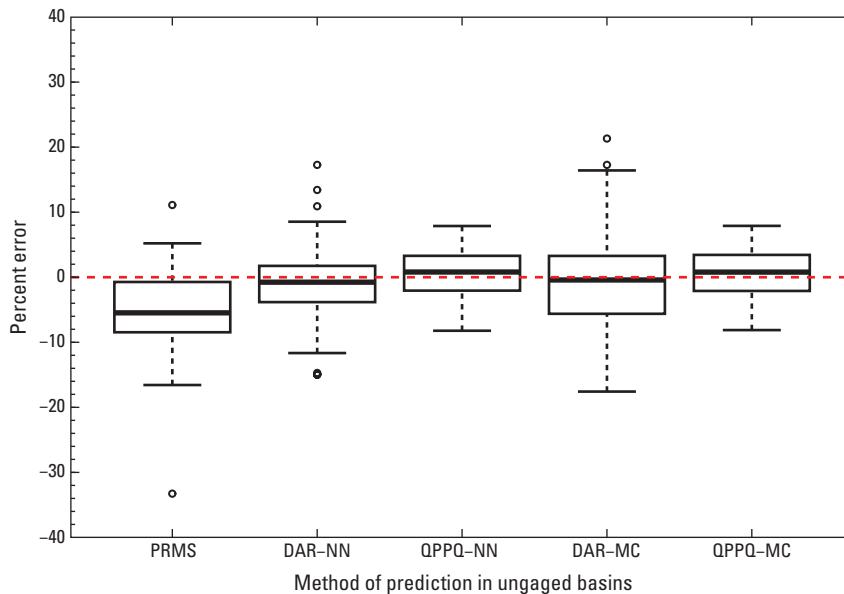


Figure 4–26. The distribution of at-site percent errors in the estimated coefficient of variation (L-CV) of daily streamflow for each method of prediction in ungaged basins (PUB) is considered here. The horizontal axis indicates each PUB method. The vertical axis shows the percent error. Unbiased methods display a median near zero and minimum variability of at-site bias. The dark line indicates the median of the distribution, the box outlines the 25th and 75th percentiles, and the whiskers extend to the data point a distance not more than 1.5 times the interquartile range away from the nearest quartile. The PUB methods include the Precipitation Runoff Modeling System (PRMS), drainage-area ratio with the nearest-neighboring index streamgauge (DAR-NN) or the map-correlated index streamgauge (DAR-MC), and nonlinear spatial interpolation using flow duration curves with the same index selection techniques (QPPQ-NN and QPPQ-MC).

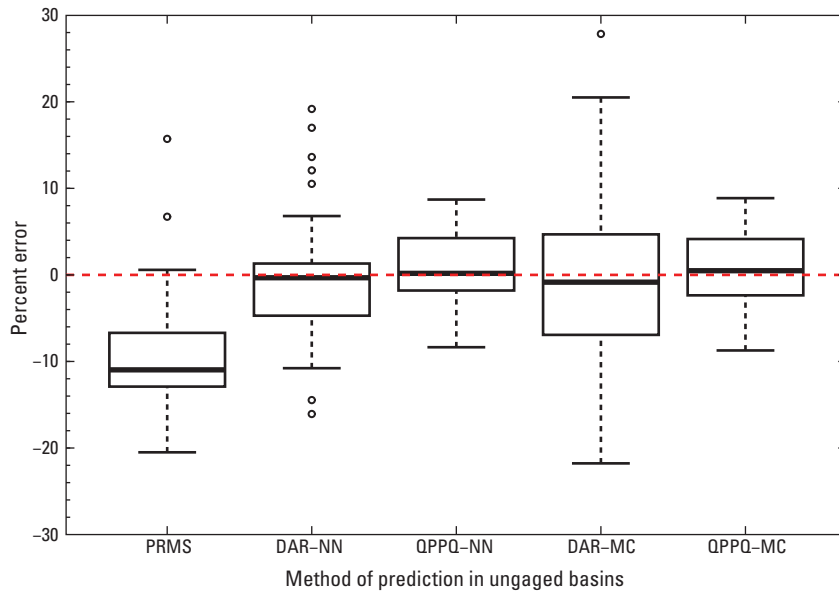


Figure 4–27. The distribution of at-site percent errors in the estimated skewness (L-skew) of daily streamflows for each method of prediction in ungaged basins (PUB) is considered here. The horizontal axis indicates each PUB method. The vertical axis shows the percent error. Unbiased methods display a median near zero and minimum variability of at-site bias. The dark line indicates the median of the distribution, the box outlines the 25th and 75th percentiles, and the whiskers extend to the data point a distance not more than 1.5 times the interquartile range away from the nearest quartile. The PUB methods include the Precipitation Runoff Modeling System (PRMS), drainage-area ratio with the nearest-neighboring index streamgage (DAR-NN) or the map-correlated index streamgage (DAR-MC), and nonlinear spatial interpolation using flow duration curves with the same index selection techniques (QPPQ-NN and QPPQ-MC).

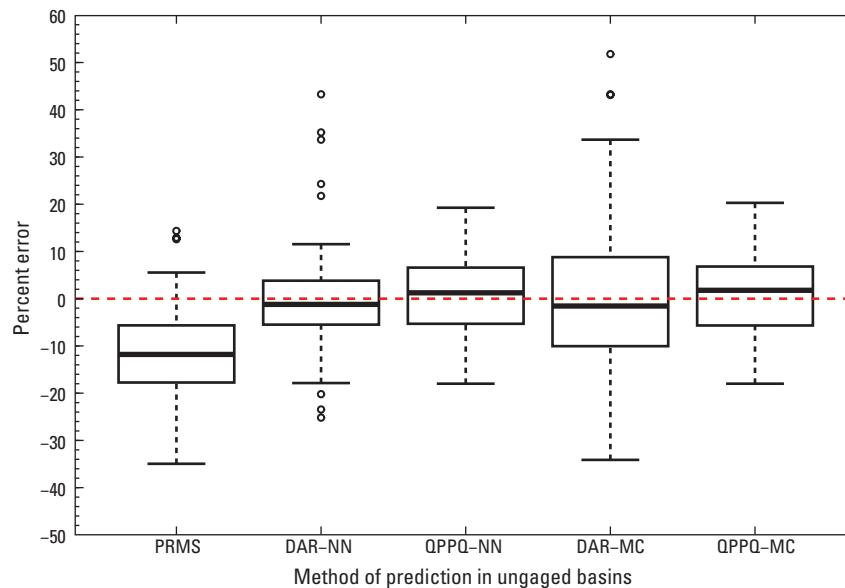


Figure 4–28. The distribution of at-site percent errors in the estimated kurtosis (L-kurtosis) of daily streamflows for each method of prediction in ungaged basins (PUB) is considered here. The horizontal axis indicates each PUB method. The vertical axis shows the percent error. Unbiased methods display a median near zero and minimum variability of at-site bias. The dark line indicates the median of the distribution, the box outlines the 25th and 75th percentiles, and the whiskers extend to the data point a distance not more than 1.5 times the interquartile range away from the nearest quartile. The PUB methods include the Precipitation Runoff Modeling System (PRMS), drainage-area ratio with the nearest-neighboring index streamgage (DAR-NN) or the map-correlated index streamgage (DAR-MC), and nonlinear spatial interpolation using flow duration curves with the same index selection techniques (QPPQ-NN and QPPQ-MC).

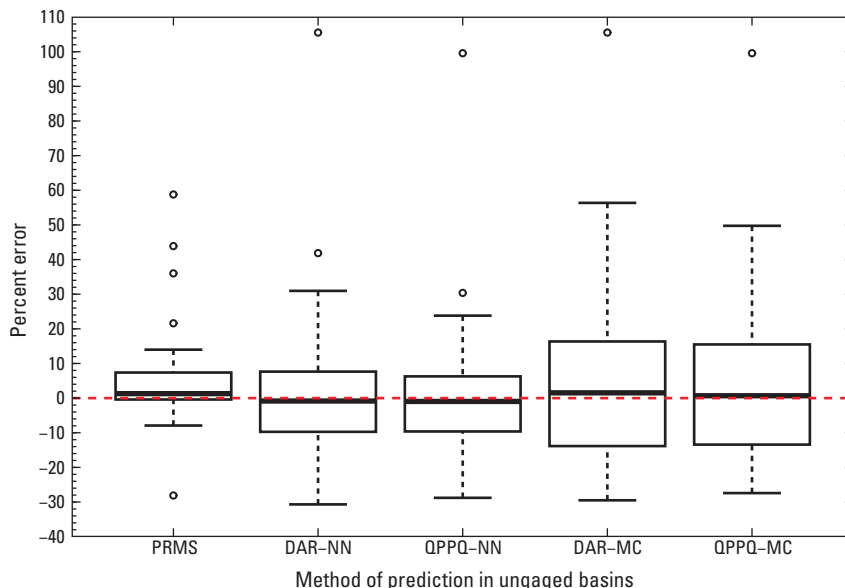


Figure 4–29. The distribution of at-site percent errors in the estimated lag-1 autocorrelation of daily streamflows for each method of prediction in ungaged basins (PUB) is considered here. The horizontal axis indicates each PUB method. The vertical axis shows the percent error. Unbiased methods display a median near zero and minimum variability of at-site bias. The dark line indicates the median of the distribution, the box outlines the 25th and 75th percentiles, and the whiskers extend to the data point a distance not more than 1.5 times the interquartile range away from the nearest quartile. The PUB methods include the Precipitation Runoff Modeling System (PRMS), drainage-area ratio with the nearest-neighboring index streamgauge (DAR-NN) or the map-correlated index streamgauge (DAR-MC), and nonlinear spatial interpolation using flow duration curves with the same index selection techniques (QPPQ-NN and QPPQ-MC).

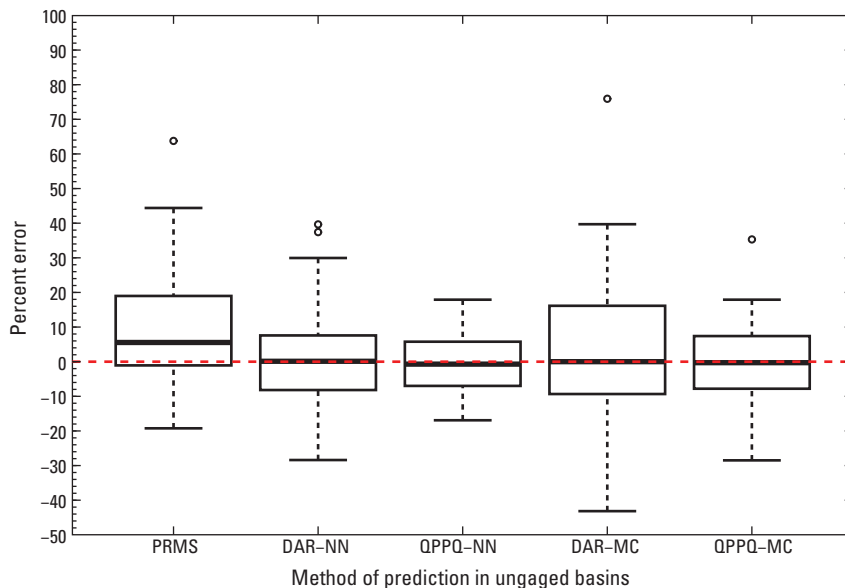


Figure 4–30. The distribution of at-site percent errors in the estimated amplitude of the sinusoidal seasonal trend of daily streamflows for each method of prediction in ungaged basins (PUB) is considered here. The horizontal axis indicates each PUB method. The vertical axis shows the percent error. Unbiased methods display a median near zero and minimum variability of at-site bias. The dark line indicates the median of the distribution, the box outlines the 25th and 75th percentiles, and the whiskers extend to the data point a distance not more than 1.5 times the interquartile range away from the nearest quartile. The PUB methods include the Precipitation Runoff Modeling System (PRMS), drainage-area ratio with the nearest-neighboring index streamgauge (DAR-NN) or the map-correlated index streamgauge (DAR-MC), and nonlinear spatial interpolation using flow duration curves with the same index selection techniques (QPPQ-NN and QPPQ-MC).

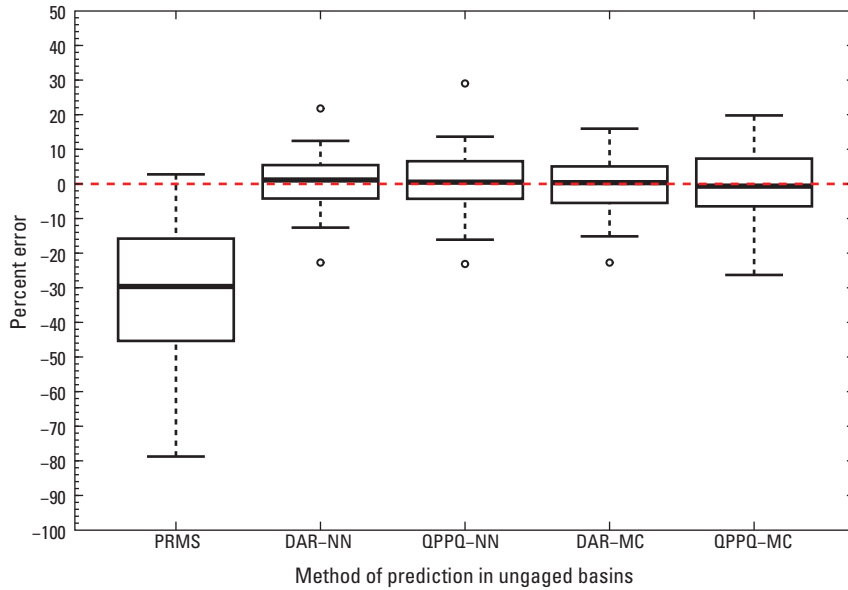


Figure 4-31. The distribution of at-site percent errors in the estimated phase of the sinusoidal seasonal trend of daily streamflows for each method of prediction in ungaged basins (PUB) is considered here. The horizontal axis indicates each PUB method. The vertical axis shows the percent error. Unbiased methods display a median near zero and minimum variability of at-site bias. The dark line indicates the median of the distribution, the box outlines the 25th and 75th percentiles, and the whiskers extend to the data point a distance not more than 1.5 times the interquartile range away from the nearest quartile. The PUB methods include the Precipitation Runoff Modeling System (PRMS), drainage-area ratio with the nearest-neighboring index streamgage (DAR-NN) or the map-correlated index streamgage (DAR-MC), and nonlinear spatial interpolation using flow duration curves with the same index selection techniques (QPPQ-NN and QPPQ-MC).

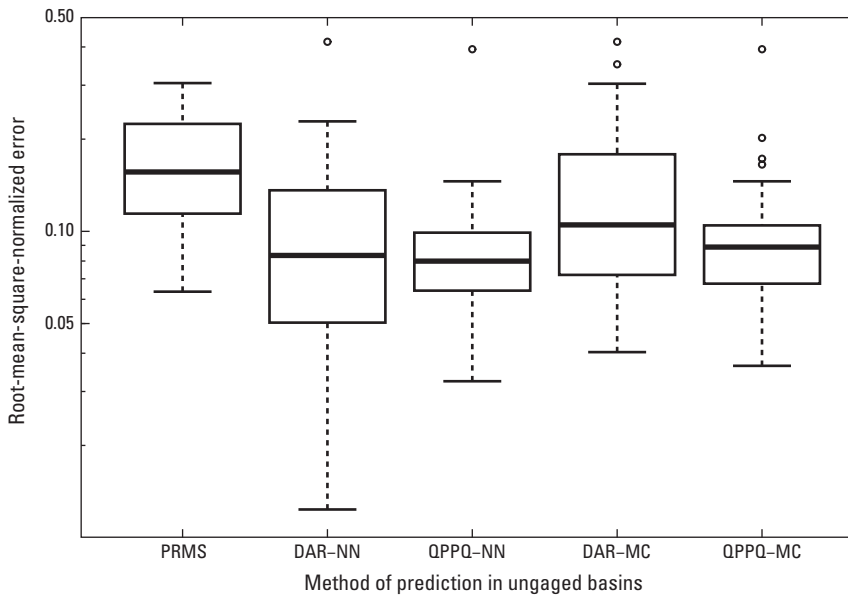


Figure 4-32. The distribution of the at-site root-mean-square-normalized errors of estimated Fundamental Daily Streamflow Statistics (FDSS) for each method of prediction in ungaged basins (PUB) is considered here. The horizontal axis indicates each PUB method. The vertical axis indicates the root-mean-square-normalized error. Lower values represent less error, on average. The dark line indicates the median of the distribution, the box outlines the 25th and 75th percentiles, and the whiskers extend to the data point a distance not more than 1.5 times the interquartile range away from the nearest quartile. The PUB methods include the Precipitation Runoff Modeling System (PRMS), drainage-area ratio with the nearest-neighboring index streamgage (DAR-NN) or the map-correlated index streamgage (DAR-MC), and nonlinear spatial interpolation using flow duration curves with the same index selection techniques (QPPQ-NN and QPPQ-MC).

Publishing support provided by:
Denver Publishing Service Center, Denver, Colorado

For more information concerning this publication, contact:
USGS Office of Surface Water
415 National Center
12201 Sunrise Valley Drive
Reston, VA 20192
(703) 648-5301

Or visit the Office of Surface Water Web site at:
<http://water.usgs.gov/osw/>

This publication is available online at:
<http://dx.doi.org/10.3133/sir20155089>

